Ultrasonics Sonochemistry 80 (2021) 105803

Contents lists available at ScienceDirect

Ultrasonics Sonochemistry

journal homepage: www.elsevier.com/locate/ultson

Dual-frequency multi-angle ultrasonic processing technology and its real-time monitoring on physicochemical properties of raw soymilk and soybean protein

Lei Zhang [a], Xue Wang [a], Yang Hu [a], Olugbenga Abiola Fakayode [a,b], Haile Ma [a], Cunshan Zhou [a,*], Zhenyuan Hu [a], Aiming Xia [c], Qun Li [c]

[a] School of Food and Biological Engineering, Jiangsu University, Zhenjiang 212013, China
[b] Department of Agricultural and Food Engineering, University of Uyo, Uyo 520001, Akwa Ibom State, Nigeria
[c] Zhenjiang New Mill Bean Industry Co. LTD, Zhenjiang 212000, China

ARTICLE INFO

Keywords:
Raw soymilk
Dual-frequency multi-angle ultrasound
Ultrasonic field monitoring
Soybean protein
Physicochemical properties

ABSTRACT

To improve the soybean protein content (SPC), flavor and quality of soymilk, the effects of dual-frequency ultrasound at different angles (40 + 20 kHz 0°, 40 + 20 kHz 30°, 40 + 20 kHz 45°) on physicochemical properties and soybean protein (SP) structure of raw soymilk were mainly studied and compared with the conventional single-frequency (40 kHz, 20 kHz) ultrasound. Furthermore, the intensity of the ultrasonic field in real-time was monitored via the oscilloscope and spectrum analyzer. The results showed that 40 + 20 kHz 45° treatment significantly increased SPC. The ultrasonic field intensity of 40 + 20 kHz 0° treatment was the largest (8.727×10^4 W/m^2) and its distribution was the most uniform. The emulsifying stability of SP reached the peak value (233.80 min), and SP also had the largest particle size and excellent thermal stability. The protein solubility of 40 + 20 kHz 30° treatment attained peak value of 87.09%. 20 kHz treatment significantly affected the flavor of okara. The whiteness and brightness of raw soymilk treated with 40 kHz were the highest and the system was stable. Hence, the action mode of ultrasonic technology can be deeply explored and the feasibility for improving the quality of soymilk can be achieved.

1. Introduction

The soybeans are cultivated widely in China. Meanwhile, several products are processed from soybeans, among which soymilk is the main product. Soymilk is the product of soybeans obtained after soaking and grinding processes with certain proportion of water. Soymilk is rich in nutrition, including plenty of protein, vitamin, soy isoflavone and other components, and also widely popular in other Asian countries [1]. Soybeans have a complete variety of protein, amino acids and essential amino acids without cholesterol [2]; however, during ground processing the ratio of soybean to water affects the ground degree of soybeans and the particle size of okara, that is, a pulp consisting of insoluble parts of the soybeans that remain after pureed soybeans are filtered in the production of soymilk and tofu. As a result, the soybean protein content (SPC) of soymilk could be severely affected: the less the water, the more insufficient grinding. Thus, soybean protein (SP) resides in okara, and SPC is low in soymilk. On the contrary, the more the water, the more adequate grinding, and the more dissolved SP; besides, soymilk particles are small, and the taste is delicate. Nevertheless, the superfluous water will also decrease SPC of soymilk. In addition, SPC is related to the beany flavor which is mainly derivatives of polyunsaturated fatty acids (PUFA) [3]. These compounds can be generated through the degradation of PUFA catalyzed by lipoxygenase (LOX) and hydroperoxyl derivatives. Afterwards, the derivatives are degraded into alcohols, aldehydes, ketones, acids, amines, and other volatile compounds with different flavor thresholds. Finally, beany flavor is induced [4]. The higher SPC tends to produce beany flavor easily [3]. Heating is a common method to remove the beany flavor with the risk of protein denaturation, while non-thermal technology can eliminate the risk by inhibiting LOX activity, and it effectively improves antioxidant properties of soybean products. Wang et al. [4] claimed that proteins with high content of lysine (Lys), arginine (Arg) and cysteine (Cys) had a stronger binding capacity to volatile compounds, and the reversible binding of covalent bonds could remove the beany flavor. In summary, an innovative non-thermal

* Corresponding author at: School of Food and Biological Engineering, Jiangsu University, 301 Xuefu Road, Jingkou District, Zhenjiang, Jiangsu 212013, China.
E-mail address: cunshanzhou@163.com (C. Zhou).

https://doi.org/10.1016/j.ultsonch.2021.105803
Received 25 September 2021; Received in revised form 15 October 2021; Accepted 18 October 2021
Available online 19 October 2021

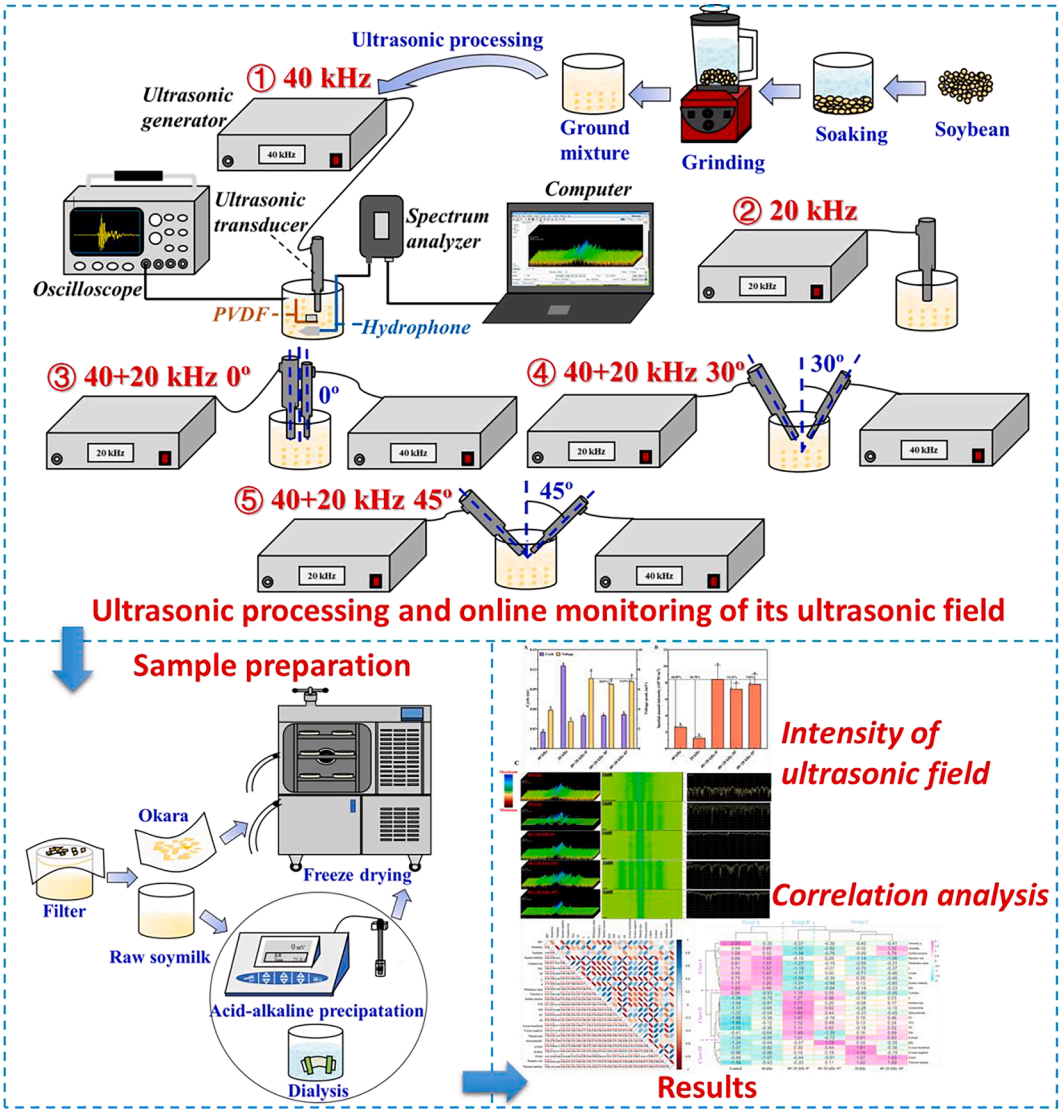

Fig. 1. Schematic graph of study.

technology is needed to improve SPC and flavor quality during soymilk processing.

As one type of non-thermal technology, ultrasound has been applied widely in food engineering. Due to green and pollution-free characteristic, ultrasound-assisted extraction has a wide application with advantages of short extraction time, high extraction rate and no chemicals residue [5–7]. The application of ultrasonic technology in protein extraction not only increases SPC and its solubility, but also induces SP structural changes [8–10]. Previous studies have shown that ultrasonic treatment can change the secondary structure of SP, resulting in a decrease of α-helix and β-sheet structure, and an increase of random coil, thus causing a relatively loose tertiary structure [11]. Compared with single-frequency ultrasound, the simultaneous action of dual-frequency ultrasound will have a synergistic effect because as the cavitation threshold is reduced, more cavitation bubbles can be generated with greater intensity. Therefore, the destruction of cell walls is accelerated, and the process of substance extraction and permeation is promoted [12–14]. Moreover, dual-frequency ultrasound can overcome the uneven phenomenon of single-frequency ultrasound [15,16]. Lian et al. [17] found that dual-frequency ultrasound could significantly increase protein kernel extracted from Chlorella. Xu et al. [18] found multi-frequency ultrasound obviously increased the degree of hydrolysis of casein. The pressure generated by ultrasonic mechanical waves drives cavitation bubbles to grow and collapse in the liquid environment, accompanied by micro-jet and elevated temperature [14].The mechanical waves in different ultrasonic frequencies are different, and the number, size, and oscillation cycles of bubbles are also different. Compared with low-frequency ultrasound, high-frequency ultrasound bubbles have narrower activity range, shorter growth cycle and smaller expandable size [19,20]. Ye et al. [14] studied the bubble dynamics of dual-frequency ultrasound, and found that bubbles oscillated simultaneously in a combined manner produced more larger bubbles and overcame the cavitation shielding. Acoustic signals in time–frequency domain were established to characterize the ultrasonic field when bubbles grew, oscillated, and collapsed [21]. Polyvinylidene fluoride (PVDF) sensor and hydrophone are commonly used to measure ultrasonic field signals [21–23], which can convert acoustic signals generated by bubble oscillation into electrical signals.

However, there are few researches on placed angles and directivity of dual-frequency ultrasound. Therefore, compared with single-frequency ultrasound (40 kHz, 20 kHz), the purpose of this study is to explore effects of dual-frequency ultrasound (40 + 20 kHz) at different angles (0°, 30°, 45°) on the physicochemical properties and flavor quality of raw soymilk. Based on different ultrasonic processing treatments, the structure and thermal stability of SP from raw soymilk were further analyzed, and acoustic signals were acquired by the online monitoring

system to reveal the ultrasonic intensity.

2. Materials and methods

2.1. Materials

The soybeans were purchased from a market (Lvliang, Shanxi, China), while corn oil was bought from a supermarket (Zhenjiang, Jiangsu, China). All other reagents were analytical grade, purchased from Sinopharm Chemical Reagent Co., Ltd. (Shanghai, China).

2.2. Preparation methods of raw soymilk

The modified method was used to prepare raw soymilk [1,24]. 280 g soybeans were soaked in tap water at a ratio of 1:4 (W/V) at 25 ± 1 °C for 10 h. Thereafter, the soaked soybeans were rinsed with deionized water for 2–3 times, and deionized water was added in the ratio of 1:8 (dry beans: water, W/V), and ground by soymilk maker (SGM-168, Chuangguan Electric Factory, Zhongshan, Guangdong, China) for 1 min at a speed of about 12,000 r/min. The ground mixture consisted of seriflux and scum; and then treated through different ultrasonic methods (Section 2.3). After filtering by two layers of gauze, raw soymilk was obtained. The okara was dried in a vacuum freeze dryer (Epsilon 2-6D LSC plus, Martin Christ, Germany) for 48 h to analyze the flavor of the raw soymilk.

2.3. Ultrasonic treatments and online monitoring methods

300 mL of the above-mentioned ground mixture was stirred evenly in the beaker at 8 ± 1 °C controlled by ice-water bath. For single-frequency ultrasonic treatment, energy-gathered ultrasonic equipment (CHEER-SONIC Ultrasonic Equipment Co., Ltd., Hangzhou, China) with single center frequency of 40 or 20 kHz was utilized. The ultrasonic frequency mode was sweeping ultrasound, sweeping amplitude was ± 1 kHz around the corresponding center frequency, and sweeping period was 100 ms. The tip diameter of the ultrasonic transducer was 0.7–1.1 cm and submerged, under 1.5 cm of liquid level in the beaker. The power of single-frequency ultrasonic treatment was 160 W. In the dual-frequency (40 + 20 kHz) multi-angle ultrasonic treatment, 40 and 20 kHz energy-gathered ultrasonic equipment were used simultaneously, and the total power was also 160 W. Two ultrasonic transducers of the equipment were placed vertically, that is, 0° away from the vertical baseline, and the space between the transducers was about 2 cm. The aforementioned ultrasonic parameters remained the same, while the angles between the transducers were changed at angles of 30° and 45° respectively deviated from the vertical baseline.

The schematic diagram of processing flow and the treated groups of raw soymilk are shown in Fig. 1 viz. single-frequency 40 kHz ultrasonic treatment (40 kHz), single-frequency 20 kHz ultrasonic treatment (20 kHz), dual-frequency 40 + 20 kHz ultrasonic treatment with 0° from vertical baseline (40 + 20 kHz 0°), dual-frequency 40 + 20 kHz ultrasonic treatment with 30° from the vertical baseline (40 + 20 kHz 30°), and dual-frequency 40 + 20 kHz ultrasonic treatment with 45° from vertical baseline (40 + 20 kHz 45°). The treatment without ultrasound was named Control. The total ultrasonic time was 20 min, and the intermittent ratio was 1:2.

According to the previous method [22], PVDF sensor (JYC1010, Jinzhou Kexin Electronic Co., Ltd., China) and hydrophone (8103, Brüel & Kjær Sound & Vibration Measurement, Denmark) were used to monitor ultrasonic signals. Signals in time domain were displayed in oscilloscope (MDO3024, Tektronix, Inc., USA), and that in frequency domain in Real-time spectrum analyzer (RSA306B, Tektronix, Inc., USA) with different color levels. All monitored ultrasonic signals were closely related to the ultrasonic field intensity. The spatial peak acoustic intensity (I, W/m^2) was calculated by Eq. (1).

$$I = \frac{U^2}{M^2 \times \rho \times c} \quad (1)$$

where U is instantaneous voltage peak (V), M is the sensitivity of PVDF with a value of 2×10^{-8} (V/Pa), ρ is the density of raw soymilk (kg/m^3), c is the sound velocity of raw soymilk about 1.5×10^3 (m/s).

2.4. Extraction methods of SP

The extraction method of SP [25–27] was slightly modified. A certain amount of deionized water was added to the aforementioned raw soymilk with ratio of 1:10 (soybean: water) and mixed adequately. Next, pH was adjusted to 8.0 with 2 M NaOH, stirred at 40 °C and 250 rpm for 2 h to fully hydrate the protein. After centrifugation with the rotated speed of 9000 r/min at 4 °C for 20 min, the supernatant was collected, adjusted to pH 4.5 by 2 M HCl, and centrifuged with the rotated speed of 6000 r/min at 4 °C for 20 min. Subsequently, the remaining precipitation was stirred again with deionized water and centrifuged with the rotated speed of 6000 r/min at 4 °C for 20 min, repeated two times. The washed protein was dialyzed (MWCO:14000D, MD:34) with deionized water at 4 °C for 72 h, while the used water was changed every 8 h. After dialysis, the protein solution was centrifuged at 6000 r/min, 4 °C for 20 min. The precipitation was collected and dispersed evenly in trace deionized water, and the pH was adjusted to 7.0 with 2 M of NaOH. Finally, the protein solution was freeze-dried for 48 h to get protein powders and stored in the refrigerator at −20 °C for analysis.

2.5. Physicochemical property determination of raw soymilk

2.5.1. SPC and solubility

SPC was determined by Coomassie brilliant blue (Bradford) method with bovine serum albumin as the standard [28]. Raw soymilk was diluted 200 times, 1 mL was taken and mixed with 5 mL 0.1 mg/mL G-250 standard solution (90% ethanol : 85% phosphoric acid : deionized water = 1:2:17, V/V/V) uniformly and reacted in the lucifugal condition for 5 min. The absorbance was measured at wavelength of 595 nm by spectrophotometer (T6NC, Beijing PUXI General Instrument Co., Ltd., Beijing, China) to represent SPC.

The determination of solubility was based on the method [29] with some modifications. The same amount of raw soymilk was centrifuged at 6000 r/min, 20 °C for 20 min to determine SPC of supernatant, and the solubility was measured by Eq. (2).

$$\text{Solubility} = \frac{S_1}{S_2} \times 100\% \quad (2)$$

where, S_1 is SPC of supernatant (mg/g), S_2 is SPC of raw soymilk (mg/g).

2.5.2. Turbidity and system stability

Turbidity was measured in accordance with the method of Li et al. [26] with modification. The raw soymilk was diluted 100 times, and deionized water was used as the blank control. The absorbance value was recorded at 600 nm, that is, turbidity.

The system stability of raw soymilk was carried out by the previous method [30]. 2 mL raw soymilk was diluted to 100 mL and centrifuged at 4000 r/min, 20 °C for 10 min. The absorbance value of the supernatant was measured at 785 nm, and deionized water was used as the blank control.

$$\text{Systemstability} = \frac{SS_1}{SS_2} \times 100\% \quad (3)$$

where SS_1 is absorbance value of supernatant, SS_2 is absorbance value of raw soymilk.

2.5.3. Conductivity, total phenol (TP) and total flavonoids (TFC)

The conductivity of raw soymilk was measured with a pen-type

conductivity meter (CT-20, Shanghai LICHEN-BX Instrument Technology Co., Ltd., Shanghai, China), which was stirred continuously until the value was stable.

Folim-ciocalfen method was used to determine TP [31], and values were expressed as equivalent per milligram of gallic acid based on dry weight (mg GAE/g).

TFC was determined by the method [32], and values were expressed as equivalent per milligram of rutin based on dry weight (mg RE/g).

2.5.4. Color

The color of raw soymilk was detected by a colorimeter (CR-400, Konica Minolta, Inc., Japan), and whiteness value was calculated according to the method of Feng et al. [33].

$$\text{Whitenessvalue} = 100 - \sqrt{(100 - L)^2 + a^2 + b^2} \quad (4)$$

where L represents brightness, a represents redness, b represents yellowness.

2.5.5. Rheological properties

Based on the method of Li et al.[34], Card-rotational rheometer (DHR-1, TA Instruments, New Castle, DE) was used to test the viscosity, storage modulus and loss modulus of raw soymilk. 40 mm parallel plate was selected with a gap of 1 mm, and the loading volume of samples was kept at 1.5 mL at 25 °C. The viscosity was carried out by variable shear rate method from 6.0 to 200 s^{-1} for 60 s. The viscoelasticity was recorded as logarithmic scanning way with oscillatory scanning mode at the frequency of 1 Hz, pressure of 1 Pa and strain range of 0.5–50%.

2.5.6. Surface tension

The surface tension of raw soymilk was tested according to the method of Du Noüy Ring [35] by automatic surface tensionmeter (QBZY-2, Shanghai Fangrui Instrument Co., Ltd., Shanghai, China). Before measurement, the platinum ring was cauterized, cooled, and calibrated with deionized water.

2.5.7. Emulsifying properties

According to the method of Zhu et al. [27], the same amount of raw soymilk was centrifuged at 1500 r/min for 20 min, 10 mL of supernatant was taken and mixed with 5 mL of corn oil in the beaker. A high-speed tissue homogenizer (T10, IKA, Germany) was used to homogenize at 7800 r/min for 2 min. Thereafter, 0.5 mL sample was immediately obtained from the bottom of the beaker and diluted to 100 mL with 0.1% (W/V) SDS solution. With 0.1% SDS solution as the blank control, the absorbance value of 500 nm was recorded at 0 min and 30 min, respectively.

$$\text{EAI} = 2T \times \frac{A_0 \times N}{C \times L \times \phi \times 1000} \quad (5)$$

$$\text{ESI} = \frac{A_0}{A_0 - A_{30}} \times t \quad (6)$$

where EAI is emulsifying activity index (m^2/g), ESI is emulsifying stability index (min), T is equal to 2.303, N is dilution multiple (200), C is SPC of the initial solution (g/mL), L is the optical path diameter of the cuvette (0.1 cm), ϕ is oil volume fraction (1/3), A_0 is the absorbance value at 0 min, A_{30} is the absorbance value at 30 min, t is the time between two measurements (30 min).

2.5.8. Foaming properties

35 mL raw soymilk was homogenized at 7800 r/min for 2 min, and then the liquid was poured into a 100 mL volumetric cylinder and the foam volume was observed at interval of 30 min [9,27].

$$\text{FC} = \frac{V_0}{35} \times 100\% \quad (7)$$

$$\text{FS} = \frac{V_{30}}{V_0} \times 100\% \quad (8)$$

where FC is foaming capacity (%), FS is foaming stability (%), V_0 is initial foam volume (mL), V_{30} is foam volume after 30 min (mL).

2.6. Test methods of flavor

The flavor was measured according to a previous method with modification [36]. 2 g freeze-dried okara was bathed in water at 40 °C for 30 min. An electronic nose device (α-Fox3000, Alpha MOS, France) with 10 sensors was used to detect the beany flavor of okara. The flushing time was set to 180 s, and the sampling time was 120 s. The types of sensitive substances of sensors included: W1C: aromatic, W5S: broadrange, W3C: aromatic, W6S: hydrogen, W5C: arom-aliph, W1S: broad-methane, W1W: sulfur-organic, W2S: broad-alcohol, W2W: sulphchlor, W3S: methane-aliph.

2.7. Test methods of SP structure

2.7.1. Particle size and zeta-potential

Freeze-dried SP was dissolved and diluted in deionized water, and the particle size and zeta-potential were detected by laser particle size analyzer (Anton Paar Litesizer 500*, Austria). The refractive indexes of protein and water were 1.45 and 1.33, respectively, with the particle absorption rate of 0.001.

2.7.2. Secondary structure

(1) Fourier transformed infrared spectroscopy (FT-IR)

The method of Huang et al.[13] was applied using Fourier transform infrared spectrometer (510A, Beijing Ruili Analytical Instrument Co., Ltd., Beijing, China). 12–13 mg of freeze-dried SP was mixed with 600 mg of dried KBr, ground and pressed. Determination range was 400–4400 cm^{-1} with 32 scanning times and 4 cm^{-1} resolution at 25 °C.

(2) Circular dichroism (CD)

Freeze-dried SP was dissolved in deionized water and diluted to 0.025 mg/mL. Circular dichroism (JASCO J-815, JASCO Corporation, Tokyo, Japan) scanning was performed and deionized water was the blank control. The scanning wavelength range, scanning speed, bandwidth, response time were 190–260 nm, 100 nm/min, 1 nm and 1 s, respectively [27]. The CD spectrum was recorded 3 times at 25 °C, and the content of secondary structure (α-helix, β-sheet, β-turn and random coil) was calculated by CD pro software.

2.7.3. Tertiary structure

(1) Fluorescence spectrum

This was performed according to the method of Xu et al. [37]. Freeze-dried SP was dissolved in deionized water at an adjusted concentration of 0.0125 mg/mL, and the fluorescence spectrum of the protein was determined by Card-F98 fluorescence spectrophotometer (Lengguang, Shanghai, China). The emission wavelength was 300–450 nm and the excitation wavelength was 280 nm. Scanning speed was 300 nm/min, scanning interval was 0.1 nm, excitation and emission bandwidth were equal to 10 nm.

(2) Ultraviolet spectrum

Freeze-dried SP was dissolved in deionized water and diluted to 0.0125 mg/mL. The UV spectrophotometer (Varian Inc., P. Alto USA) was used for spectral scanning at 190–350 nm, and the wavelength

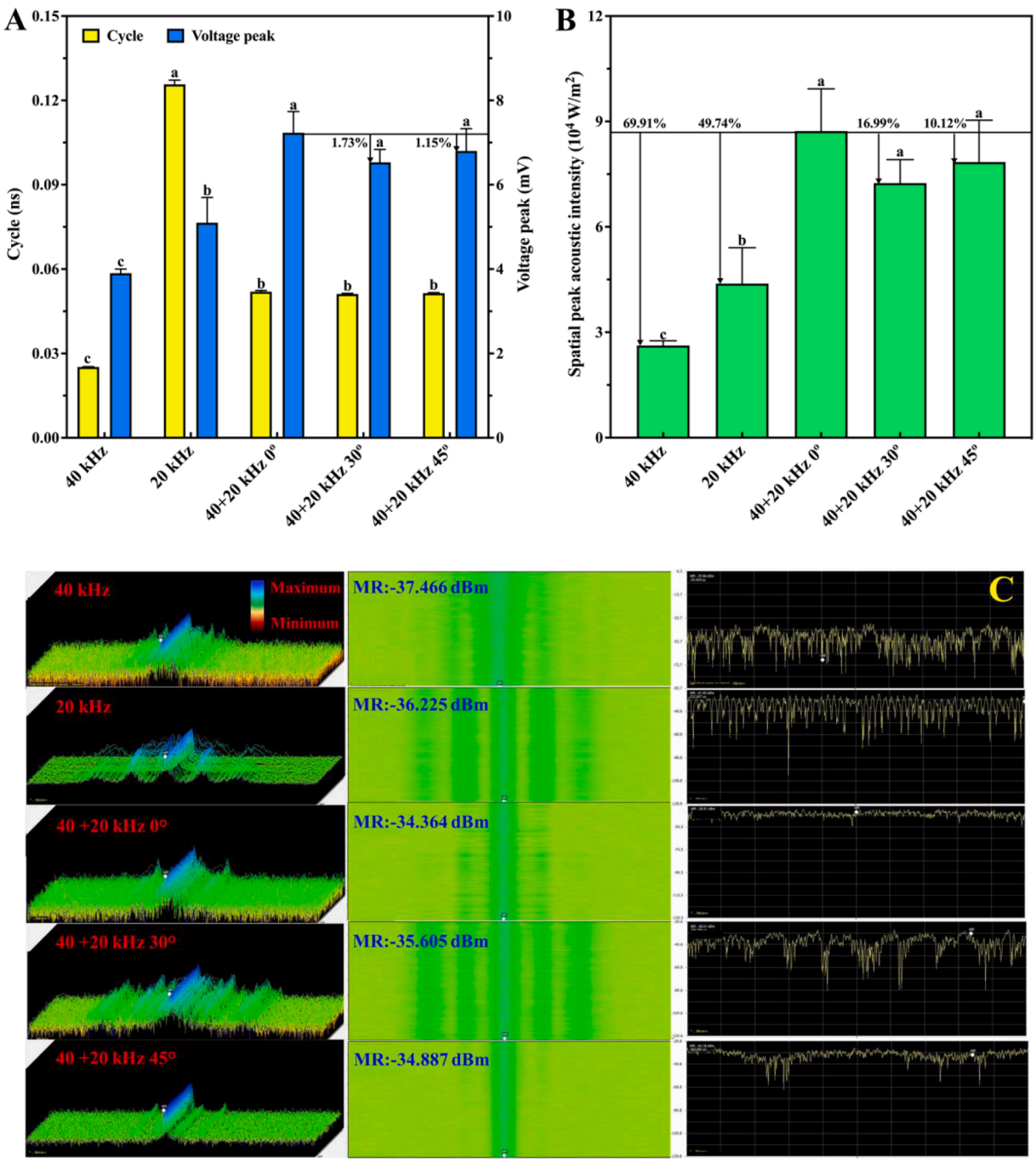

Fig. 2. Monitoring of ultrasonic field intensity during ultrasonic treatments of raw soymilk. (A) Oscillation cycle of cavitation bubbles and voltage peak, (B) Spatial peak acoustic intensity, and (C) Three-dimensional distribution of ultrasonic field intensity, DPX digital fluorescence spectrum of ultrasonic field intensity and average spectrum amplitude of ultrasonic field.

interval was 2 nm.

2.7.4. Microstructure analysis

The microstructure of SP was observed by scanning electron microscopy (S-3400 N, Hitachi Ltd., Japan) (SEM) at magnification of 850. Samples were fixed with conductive adhesive and treated by gold spraying. Samples were observed under an accelerated voltage of 15 kV.

2.7.5. Thermogravimetric analysis

Based on the method of Feng et al. [33], thermal stability of SP was measured by TG/DTA analyzer (STA 499C, Netzsch Gerätebau, Germany). 5 mg sample was placed in an alumina crucible with temperature range of 35–600 °C. Nitrogen was the carrier (50 mL/min) at a heating rate of 10 °C/min. Different thermogravimetric curves (TG) were drawn with the first derivative (DTG).

2.8. Statistical analysis

All experiments were conducted at least three times and results were presented as mean ± standard deviation. One-way analysis of variance (ANOVA) and Duncan's test ($p < 0.05$) were processed by SPSS 26.0 software (SPSS Inc., Chicago, IL, USA). The graphs were drawn by Prism 8 (GraphPad Inc., USA) and Origin 2018 (OriginLab Corporation., Northampton, MA, USA). Pearson's correlation coefficient analysis was

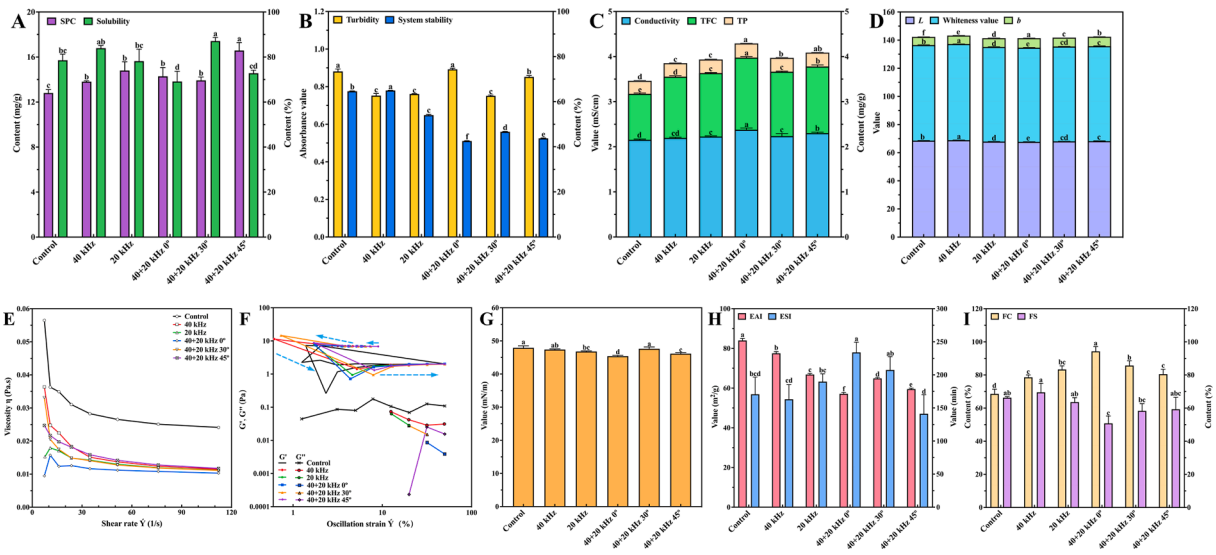

Fig. 3. Effects of different ultrasonic treatments on physicochemical properties of raw soymilk. (A) SPC and solubility, (B) Turbidity and system stability, (C) Conductivity, TP and TFC, (D) Color character, (E) Rheological properties, (F) G' and G'', (G) Surface intension, (H) EAI and ESI, and (I) FC and FS.

implemented by corrplot package in R version 4.1.0 (R Foundation for Statistical Computing, Vienna, Austria).

3. Results and discussion

3.1. Online monitoring of ultrasonic field intensity during raw soymilk treated

During ultrasonic treated process of raw soymilk, oscilloscope and spectrum analyzer were introduced to monitor oscillation cycle of cavitation bubbles, the intensity and distribution of ultrasonic field in time–frequency domain, as shown in Fig. 2. Fig. 2A shows oscillation cycle of cavitation bubbles and the ultrasonic intensity represented by voltage peak in time domain. Different ultrasonic frequencies had different oscillation cycles. The oscillation cycle of 20 kHz treatment was the longest, about 0.1257 ns, which was more than two times of dual-frequency ultrasonic treatment; while the oscillation cycle of 40 kHz treatment was the shortest, about 0.0252 ns. The lower the ultrasonic frequency, the longer the oscillation cycle, and the bigger the bubble radius, which induced stronger mechanical waves and significant cavitation effect. The study [19] showed that high ultrasonic frequency caused the narrow activity space of cavitation bubbles and reduced their radius. It was also reported that strong shock waves were generated at low ultrasonic frequency because the collapse time and expansion size of cavitation bubbles were increased [20]. Cavitation effects were derived from the oscillation process of cavitation bubbles. The instantaneous pressure generated as bubbles collapse, acted on the surface of PVDF sensor, and then the mechanical energy was converted into electrical energy (voltage peak), which was used to represent the ultrasonic intensity [22]. Results showed that the voltage peak of dual-frequency ultrasonic treatment was significantly higher than that of single-frequency; thereinto, the voltage peak of 40 + 20 kHz 0° treatment was the highest, reaching 7.23 mV, and the ultrasonic intensity also was the strongest. The pressure generated as cavitation bubbles collapse reflected the intensity of cavitation effect, the higher the pressure, the stronger the cavitation effect [14]. Fig. 2B shows that the value of spatial peak acoustic intensity of 40 + 20 kHz 0° treatment is also the highest, which further indicates the cavitation effect was the strongest.

Fig. 2C shows the visualized distribution of ultrasonic field in frequency domain. The first column of Fig. 2C is the three-dimensional energy waterfall plot of the ultrasonic field intensity. According to the energy color levels, the intensity peak (blue) of 40 kHz treatment was the weakest intensity peak, and that of 20 kHz treatment was higher with many impurity peaks. However, the intensity peak was concentrated in the middle of 40 + 20 kHz 0° treatment with fewer impurity peaks on both sides, and the distribution of ultrasonic field was uniform, indicating that dual-frequency ultrasonic treatment is suitable for the processing of raw soymilk. The second column of Fig. 2C shows the DPX digital fluorescence spectrum of ultrasonic field intensity. Monitored multiple spectrums in a short period of time were performed by Fast Fourier Transform (FFT) and displayed in the image form. Results also revealed that the peak intensity of 40 + 20 kHz 0° treatment was concentrated (green band in the middle) with a wide range of −34.364 dBm, and 5.42%-9.03% higher than others. The third column in Fig. 2C is the average spectrum amplitude of ultrasonic field. It was discovered that the amplitude fluctuation of dual-frequency ultrasonic treatment was much smaller than single-frequency, and that of 40 + 20 kHz 0° treatment was the smallest with the most uniform distribution. In conclusion, monitoring of ultrasonic field intensity in time–frequency domain showed that the ultrasonic intensity of 40 + 20 kHz 0° treatment was the strongest with the most even distribution.

3.2. Effects of different ultrasonic treatments on physicochemical properties of raw soymilk

3.2.1. SPC and solubility

Soybeans had high SPC, and was the main source of functional plant protein that was considered as one of the most important nutritional indicators of soymilk [38]. Fig. 3A shows SPC of raw soymilk after all ultrasonic treatments increased compared with Control ($p < 0.05$). SPC of 40 + 20 kHz 45° treatment was the highest, 16.07% higher than that of 40 + 20 kHz 0° and 19.02% higher than 40 + 20 kHz 30°. Moreover, SPC of dual-frequency ultrasound was higher than single-frequency. For example, SPC of 40 + 20 kHz 45° treatment was 20.01% higher than that of 40 kHz treatment, and 12.05% higher than that of 20 kHz treatment. This was because cavitation bubbles generated by high frequency ultrasound was used as the bubble core for low frequency ultrasound to produce stronger cavitation in dual-frequency ultrasound, and the induced huge shear force increased the amount of protein extracted from okara [39]. Therefore, 40 + 20 kHz 45° treatment was the optimal ultrasound treatment to improve SPC.

Solubility which reflected the degree of dispersion, aggregation or denaturation of proteins, further affected other properties of raw soymilk, such as turbidity, system stability, and foaming properties, etc. [9].

In Fig. 3A, compared with Control, 40 kHz and 20 kHz treatment had no effect on protein solubility. However, the solubility was affected by dual-frequency ultrasonic treatments with first increased and then decreased trend based on the increment of angles. To be more specific, the solubility of 40 + 20 kHz 0° treatment was 69.14%, that of 40 + 20 kHz 30° treatment reached the peak of 87.09%, and then reduced to 72.78% after 40 + 20 kHz 45° treatment. Because shear force formed by appropriate ultrasonic treatment intensity made the molecular structure of SP loose and diminished, the solubility was improved. In addition, the turbulence induced by ultrasonic cavitation effect promoted the exposure of the charged groups in raw soymilk. Thus, the increasing interaction between protein and water was beneficial to the solubility [40]. Nevertheless, if the ultrasonic field intensity is unduly strong, the denaturation and aggregation of protein occur, and the solubility decreases [9,41].

3.2.2. Turbidity and system stability

Turbidity, the hindered degree of suspended solids to light transmission, represents the aggregation degree of protein in raw soymilk [41]. In Fig. 3B, the turbidity after ultrasonic treatment is generally lower than the Control, which is opposite to the solubility (Fig. 3A). The shear force formed by ultrasonic cavitation destroyed protein aggregation, increased solubility, reduced the hindered degree, and decreased turbidity ultimately [42]. However, strong ultrasonic intensity of 40 + 20 kHz 0° and 40 + 20 kHz 45° (Fig. 2) made the protein molecules denatured or reaggregated to new aggregation, so the turbidity increased. Similar phenomena were also observed in other study [43].

Fig. 3B also displays the system stability of raw soymilk. Under the action of the centrifugal field, the settling velocity was proportional to the square of particle radius [44]. The smaller the particle radius, the slower the settling velocity and particles suspended in the supernatant after centrifugation, which increased the system stability [45]. Compared with the Control, the stability of the remaining ultrasonic treatments decreased, except that of 40 kHz treatment which increased by 0.51%. The stability of 40 + 20 kHz 0° and 40 + 20 kHz 45° treatments decreased by 34.15% and 32.34%, respectively. Combined with the turbidity, it further proved that the stronger the ultrasonic field intensity, the greater the aggregation degree of protein with the large and precipitated particles, so the system stability reduced. This result was also proved by an earlier study [46].

3.2.3. Conductivity, TP and TFC

If the walls of soybean cells are ruptured, contents might flow out and the wall-broken rate could be assessed by the conductivity. After ultrasonic treatments, the conductivity, TP and TFC of raw soymilk significantly increased, and that of dual-frequency ultrasonic treatment was higher than single-frequency in Fig. 3C. In combination with monitoring results of ultrasonic field intensity above (Section 3.1), the intensity of dual-frequency ultrasonic field was apparently higher than single-frequency. The huge shear force formed by ultrasonic cavitation destroyed the cell wall [47], contents flowed out greatly, and the conductivity, TP and TFC were improved. Dual-frequency ultrasonic treatment was appropriate for the extraction of functional elements in foods. Ultrasonic treatment promoted the production of hydroxyl radicals and hydroxylation of benzene rings of phenolic compounds, resulting in more phenolic compounds [48]. However, ultrasonic cavitation might also promote the formation of free radicals, and reduced bioactive compounds [49]. As a result, the TP of 40 + 20 kHz 30° treatment decreased, but was still higher than that of single-frequency ultrasonic treatment ($p < 0.05$).

3.2.4. Color

Color was one of the important indicators to characterize the quality of raw soymilk. In Fig. 3D, brightness and whiteness values of raw soymilk decreased apparently after ultrasonic treatments, but yellowness values increased ($p < 0.05$): especially 40 + 20 kHz 0° treatment with the strongest ultrasonic field intensity (Fig. 2A-B). This might be attributed to the presence of pigment such as polyphenols and flavonoids or the influence of factors such as browning [46]. Section 3.2.3 shows that excessive ultrasonic cavitation promoted the formation of free radicals and the combination of phenolic substances in raw soymilk with oxygen. So, the browning of raw soymilk happened, that is, enzymatic browning. This was similar to the result of [50], free radicals induced by ultrasound triggered a series of changes related to wine chroma, leading to a higher browning index of wine. In addition, it also showed that ultrasonic treatment promoted the decomposition of colored substances [51]. The study found that ultrasound changed *L*, *a*, and *b* of strawberry juice, because the shear force and micro-jet formed by ultrasound could destroy cells, release intracellular compounds and affect color properties [52]. The effect of ultrasonic treatment on the color of plant tissues was studied by Flores-Jiménez et al.[53], during the metabolite extraction process, plant tissues were damaged and color change appeared due to synergistic effect of the erosion, shear force, sonoporation, fragmentation, capillary effect and detexturation.

3.2.5. Rheological properties

From Fig. 3E, the apparent viscosity of raw soymilk decreased with the increase of shear rate, showing shear thinning characteristic of pseudoplastic fluid [54]. In addition, compared with the Control, the viscosity of raw soymilk decreased after ultrasonic treatments, and the viscosity of 40 + 20 kHz 0° treatment was the lowest. This was caused by the strong ultrasonic cavitation (Fig. 2), in which some SP molecules were denatured, and the original gel capacity of the protein was destroyed, thus the viscosity decreased [55]. Dissanayake et al. [56] found that the increase of double electric folding between particles and the potential, secondary electroviscous effects was enhanced, and the viscosity of whey protein increased. The ultrasonic intensity of 40 + 20 kHz 45° treatment was equivalent to that of 40 + 20 kHz 0° treatment (Fig. 2A-B), but SPC of raw soymilk obtained by the former treatment was higher (Fig. 3A). In the circumstances, the denaturation and aggregation of proteins were most susceptible to occurring, the secondary electroviscous effects increased significantly, and the viscosity became higher.

Effects of different ultrasonic treatments on the storage modulus (G') and loss modulus (G'') of raw soymilk are shown in Fig. 3F, and the dotted lines in the graph represent the change path of G'. On one hand, G' was higher than G'', indicating that the oscillation characteristics of raw soymilk were mainly elastic characteristics with gel formation behavior [57]. Reducing strain curve of G' was under the previous increasing curve, the hysteresis curve was generated, further showing that the rheological behavior of raw soymilk was time-dependent shear thinning. This kind of rheological behavior could recover to a certain gel level with shear-free, which was helpful to produce tofu later [58]. On the other hand, after ultrasonic treatments, G' of raw soymilk did not change but G'' decreased, so ultrasound had impacts on the gel network structure of raw soymilk.

3.2.6. Surface tension

Surface tension was defined as the force parallel to the liquid–air surface and angles between the force and any line with unit length on the surface were right [35], which was related to solubility of proteins. From Fig. 3G, the surface tension of raw soymilk decreased after ultrasonic treatments, especially for 40 + 20 kHz 0° and 40 + 20 kHz 45° treatments, and the surface tension decreased by 5.27% and 3.33%, respectively. Combined with the solubility (Fig. 3A), it might be that the excessive ultrasonic treatment resulted in protein with denaturation, aggregation, and rearrangement, leading to a decrease of surface tension [59]. Amine et al. [60] claimed that the surface tension was also related to the charge carried by proteins; for instance, the surface tension of pea and potato proteins at pH = 10 was smaller than that at pH = 7, the number of charges carried by proteins was changed at pH = 10 and electrostatic repulsion increased.

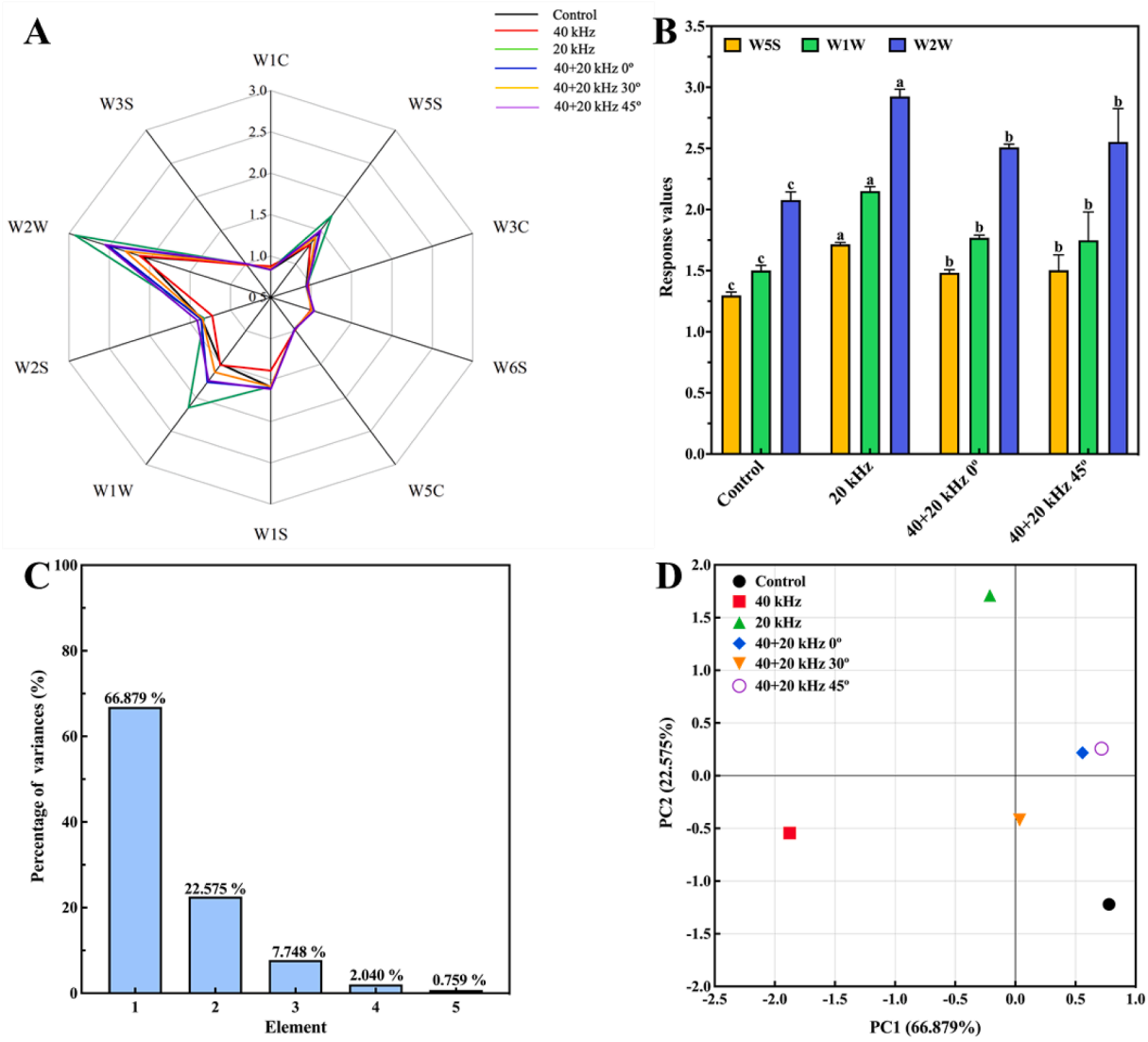

Fig. 4. Effects of different ultrasonic treatments on flavor of okara. (A) Radar map, (B) Comparison of values of W5S, W1W and W2W sensors after 20 kHz, 40 + 20 kHz 0° and 40 + 20 kHz 45°, (C) and (D) Principal component analysis.

3.2.7. *EAI and ESI*

In Fig. 3H, EAI of raw soymilk decreased after ultrasonic treatments ($p < 0.05$), especially that of 40 + 20 kHz 0° treatment which decreased from 84.007 to 57.135 m^2/g compared with the Control. EAI was associated with solubility of proteins, unfolding, aggregation degree and particle size. It was reported that high solubility could promote the diffusion of oil–water interface and EAI increased [40]. The unfolding of globular amaranth isolated proteins was promoted by high-intensity ultrasonic treatment, and the nonpolar groups were exposed with the increment of surface activity [43]. The study found that ultrasonic treatment improved emulsification properties by reducing particle size of pea proteins [61]. Meanwhile, the particle size of proteins affected EAI, the smaller the proteins, the easier the diffusing, and EAI increased [62]. Here, EAI of raw soymilk reduced, the reason might be that strong ultrasonic cavitation made SP denatured and aggregated into larger particles. The solubility of proteins reduced, some nonpolar groups were buried, and hydrophilic group were exposed. Thus, lipid droplets could not be easily attached to proteins, and EAI decreased. Compared with the Control, ESI after ultrasonic treatments increased slightly, and reached the peak of 233.980 min after 40 + 20 kHz 0° treatment. The shear force and micro-jet caused by ultrasonic cavitation, not only let proteins adsorbed and accumulated to form a viscoelastic film, but also changed the protein structure. Changes of structure led to the increase of viscoelasticity of the film, which enhanced the interaction between proteins and lipids, and ESI increased [40].

3.2.8. *FC and FS*

FC was defined as the ability of proteins to form bubbles by reducing the surface tension of the air–water interface, and FS referred to the ability of proteins to maintain foam stability. In Fig. 3I, compared with the Control, ultrasonic treatments increased FC of raw soymilk, and the maximum FC reached 94.28% after 40 + 20 kHz 0° treatment. That was because the apparent viscosity (Fig. 3E) and surface tension (Fig. 3G) of raw soymilk decreased, which provided little resistance to bubble formation and reduced cavitation threshold, and it was easier to produce cavitation bubbles as well as cavitation effect [63]. Previous study had also shown that ultrasonic treatment increased foaming properties [64]. Ultrasonic cavitation induced partial unfolding of protein structure, enhanced adsorption capacity rapidly at air–water interface, and increased FC [64,65]. Proteins of raw soymilk could better unfold and disperse at the air–water interface, so FC increased. It was claimed that ultrasonic cavitation caused partial structural changes of proteins, more flexible proteins in aqueous solution were formed, and the interaction of air–water interface and FC increased. FS depended on the thickness of

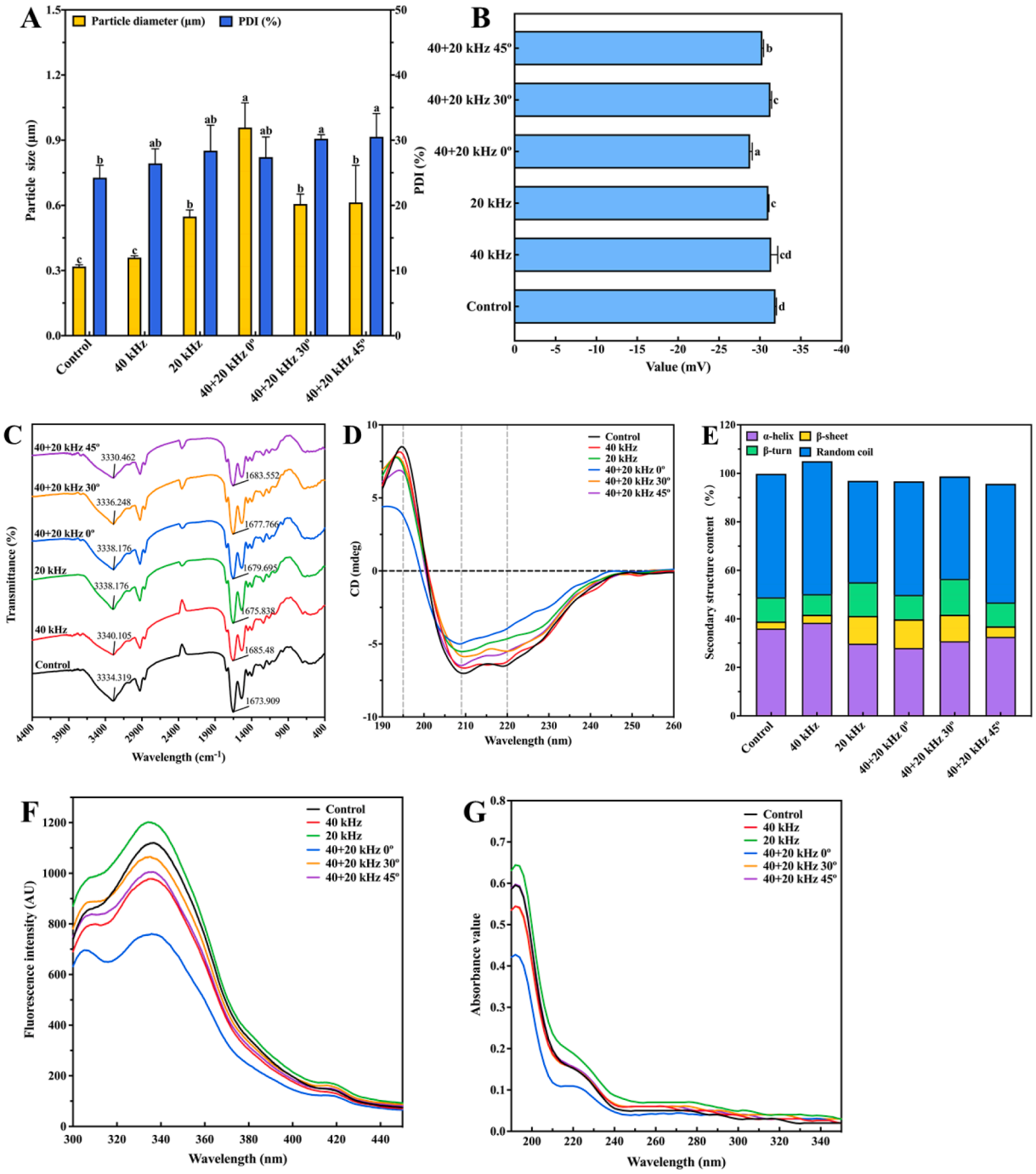

Fig. 5. Effects of different ultrasonic treatments on structural characteristics of SP. (A) Particle size and polydispersity index, (B) Zeta-potential, (C) FT-IR, (D) CD, (E) Secondary structure content, (F) Fluorescence spectrum, (G) Ultraviolet spectrum, (H) Microstructure, (I) TG, and (J) DTG.

the cohesive layer formed around bubbles [53], which was related to the solubility of proteins. If the solubility increased, SPC involved in film formation increased. Further, the interaction between protein molecules made the adsorption film more compact and thicker, so that generated bubbles could hardly rupture, and FS increased. Combined with results in Fig. 3A, the solubility was lowest after 40 + 20 kHz 0° treatment, and FS was also the lowest.

3.3. Flavor properties

The electronic nose was used to establish a radar map on response values of volatile components in okara after different ultrasonic treatments, and types of sensitive substances of different sensors were analyzed in Fig. 4A. W5S, W1W and W2W sensors had higher response values, especially after 20 kHz, 40 + 20 kHz 0° and 40 + 20 kHz 45° treatments, which indicated ultrasonic treatments promoted the generation of some nitrogen oxides, organic sulfur compounds and aromatic compounds. Other response values were almost identical and overlapped. Aromatic compounds of sensitive substances were beneficial to components of okara flavor, but nitrogen oxides and organic sulfides had negative effects on flavor. According to Fig. 4B, compared with the Control, response values of W5S, W1W and W2W sensors increased after

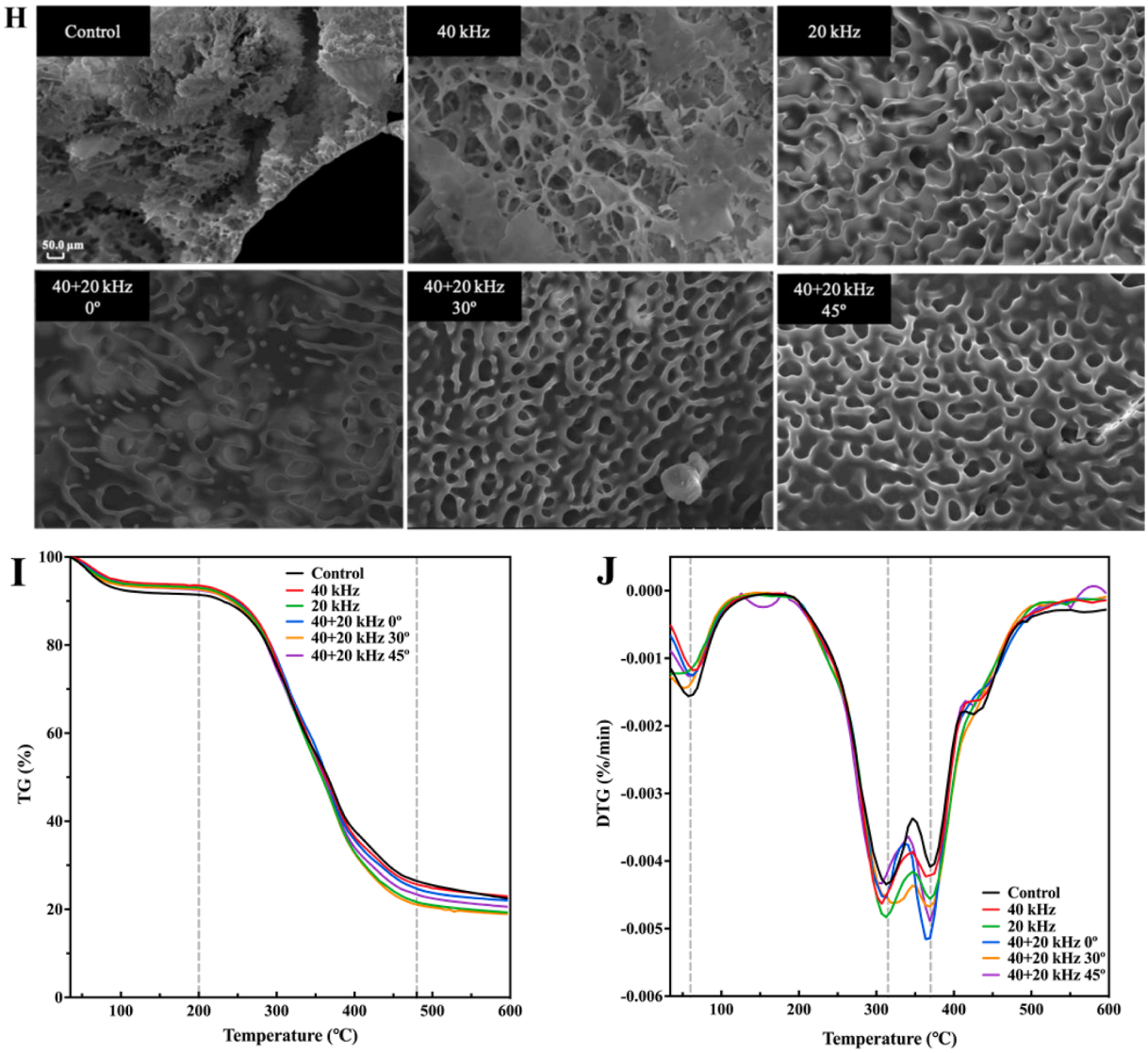

Fig. 5. (*continued*).

20 kHz treatment ($p < 0.05$), of which aromatic compounds representing beneficial components increased by about 40.76%, while nitrogen oxides and organic sulfides representing negative effects increased by about 75.45%. Therefore, although Fig. 4A shows that 20 kHz treatment had the greatest influence on okara flavor, Fig. 4B shows that 20 kHz treatment had more obvious impact on adverse flavor. In contrast, negative components measured by the electronic nose after 40 + 20 kHz 0° and 40 + 20 kHz 45° treatments were far less than that of 20 kHz treatment, thus improving okara flavor. Results all indicated that ultrasonic treatments had effects on the flavor of okara. It was observed that changes of response values after ultrasonic treatments was attributed to the chemical change in the process [66]. It was reported that legume proteins could interact with flavoring components, leading to changes in aroma characteristics [67]. Proteins could bind or absorb flavor compounds of foods, causing flavor changes during eating. [68] The flavor of okara was changed after ultrasonic treatments. Conformations of SP were changed, some internal groups were exposed, and even proteins denatured. Finally, the bond of SP was broken, and the flavor was changed with some volatile elements such as nitrogen oxides, organic sulfur, and aromatic compounds.

Principal component analysis was conducted based on electronic nose results of okara with different ultrasonic treatments. Fig. 4C shows that the sum of principal component 1 and principal component 2 was equal to 89.454%, greater than 85%, which can reflect the principal component data [66]. Therefore, principal component 1 and principal component 2 were selected to analyze the flavor of okara with different ultrasonic treatments. Fig. 4D shows that compared with the Control, ultrasonic treatments significantly change okara flavor. The positions of 40 + 20 kHz 0° and 40 + 20 kHz 45° treatments were similar, and there was no difference in flavor between the two treatments. This was consistent with results of the previous radar map (Fig. 4A), and their intensity of ultrasonic field was also similar (Fig. 2A-B). However, there were significant differences between 1 and 2 principal components of okara in 20 kHz treatment and the Control, so 20 kHz treatment had the greatest influence on the okara flavor, which was consistent with the results of the radar map [69].

3.4. Structural characteristics of SP

3.4.1. Particle size, polydispersity index and zeta-potential

In Fig. 5A, the polydispersity index of protein solution was<30%, indicating that SP dispersed evenly [61,70], and the carrier system was stable. Compared with the Control, the particle size of proteins after ultrasonic treatments increased significantly ($p < 0.05$). In particular, the particle size after 40 + 20 kHz 0° treatment was the largest with the increment from 0.319 to 0.958 μm. The corresponding protein solubility

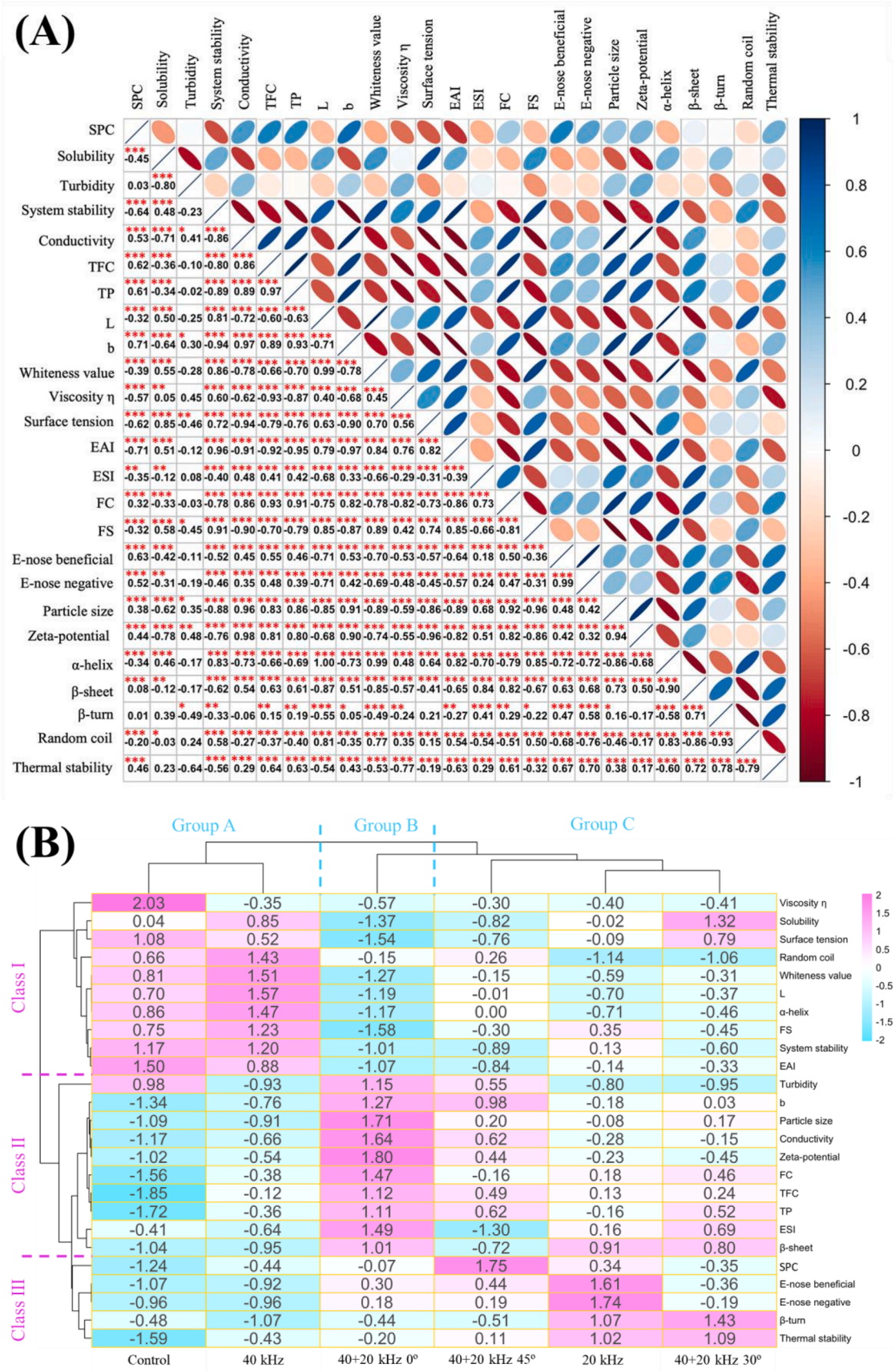

Fig. 6. Analysis of correlation (A) and clustering heat map (B) between corresponding indexes of different ultrasonic treatments. Fig. 6A visualizes the correlation between color and ellipse size, with blue representing positive correlation and red representing negative correlation. The size and color intensity of the upper triangle ellipse are positively proportional to the correlation coefficient. The lower triangle represents the correlation coefficient, which is marked as significant ($p < 0.05$ (*), $p < 0.01$ (**), $p < 0.001$ (**)). In Fig. 6B, blue represents the lowest content, while red represents the highest content.

was the smallest (Fig. 3A). Ultrasonic treatments resulted in the increment of protein particle size and decrement of protein solubility, which was caused by the denaturation and aggregation of proteins to form larger particles due to ultrasonic cavitation [9]. It was reported that ultrasonic turbulence and micro-jet could accelerate the collision and aggregation of protein particles, resulting in the increment of particle size with the formation of unstable aggregates [43]. Furthermore, high-intensity ultrasound or prolonged overprocessing also made mass denatured proteins to accumulate.

Zeta-potential is a direct indicator of the surface charge density of charged particles [62], which is used to demonstrate the stability of colloidal system and the electrostatic interaction between particles [25]. As shown in Fig. 5B, potentials were all negative, indicating that the negative charges on the surface of SP were higher than the positive charges, and the net charges were negative. Compared with the Control, absolute charges after 40 + 20 kHz 0° treatment decreased significantly ($p < 0.05$). It was reported that protein aggregations formed by high power ultrasound also reduced absolute charges [71]. Here, the reduction of absolute charges might be related to protein denaturation and aggregation to form large particles after ultrasonic treatments.

3.4.2. FT-IR and CD

The characteristic bond or group of protein molecule was displayed by the wavelength of absorption bands in the infrared spectrum [8]. Changes of proteins were analyzed by special absorption wavelengths of amide A band (3400–3200 cm^{-1}), amide I band (1700–1600 cm^{-1}), amide II band (1550–1530 cm^{-1}) and amide III band (1300–1200 cm^{-1}). Among them, amide A band was due to N–H stretching vibration, amide I band was related to C = O, C-N stretching vibration, amide II band was mainly caused by N–H stretching vibration and C-N deformation, and amide III band was related to C-N stretching and N–H bending [8,72,73]. In Fig. 5C, it was found that after ultrasonic treatments, the absorption peaks at 3334.319 cm^{-1} and 1673.909 cm^{-1} (Control) changed to 3340.105 cm^{-1} and 1685.48 cm^{-1} (40 kHz), 3338.176 cm^{-1} and 1675.838 cm^{-1} (20 kHz), 3338.176 cm^{-1} and 1699.695 cm^{-1} (40 + 20 kHz 0°), 3336.248 cm^{-1} and 1677.766 cm^{-1} (40 + 20 kHz 30°), and 3340.462 cm^{-1} and 1683.552 cm^{-1} (40 + 20 kHz 45°), respectively. It was observed that different ultrasonic treatments have different effects on the secondary structure of SP.

Effects of different ultrasonic treatments on secondary structure α-helix, β-sheet, β-turn and random coil of SP were studied in Fig. 5D. SP was a typical α + β type protein structure, with a positive absorption peak at 195 nm and two negative absorption peaks at 209 and 220 nm [40]. Ultrasonic treatments changed the secondary structure of SP. After 40 + 20 kHz 0° treatment, the absorption peak intensity at 195, 209 and 220 nm gradually decreased, and the wavelength of positive absorption peak shifted blue, indicating some changes in the secondary structure of SP. Contents of α -helix, β-sheet, β-turn and random coil are shown in Fig. 5E. Compared with the Control, α-helix of SP after 40 + 20 kHz 0° treatment decreased, while β-sheet increased, which was related to protein aggregation [17], and it was consistent with results that SP had the largest particle size after 40 + 20 kHz 0° treatment (Fig. 5A). Changes in protein secondary structure not only depended on amino acid sequences, but also were related to intermolecular interactions [40]. In this study, different ultrasonic treatments led to the decrement of α-helix and increment of β-sheet, due to the shear force and micro-jet caused by ultrasonic cavitation. Hence, the protein–protein interaction was destroyed, denaturation and aggregation of proteins occurred, leading to the difference of secondary structures conformation.

3.4.3. Fluorescence spectrum and ultraviolet spectrum

Fluorescence and ultraviolet spectrums reflected the protein change of tertiary structure, mainly the exposure of tryptophan (Trp), tyrosine (Tyr) and phenylalanine (Phe) residues [17,41]. In Fig. 5F-G, compared with the Control, the fluorescence and ultraviolet spectrum absorption peaks of proteins treated by 20 kHz increased significantly. After 40 + 20 kHz 0° treatment, absorption peaks were the smallest, and the damage degree of tertiary structure of proteins was the largest, the same as results of CD (Fig. 5D), and the intensity of ultrasonic field was the strongest (Fig. 2A-B). Protein particles could be broken into single small molecules by ultrasound, which increased the vibration degree and stimulated stronger fluorescence [29]. It was reported that ultrasonic cavitation stretched protein molecules, changed spatial conformation and exposed hidden hydrophobic groups, leading to the increment of fluorescence intensity [8]. In addition, ultrasound may also take Trp residues away from fluorescence quenching components such as disulfide bonds, resulting in the increment of fluorescence intensity. It was reported that ultrasound promoted soy isolate protein to unfold and expose Trp residues, resulting in the increment of fluorescence intensity [40]. The huge shear force generated by ultrasonic cavitation promoted SP to aggregate and agglomerate into larger particles, which changed the original conformation. This might cause hydrophobic groups to be buried and Trp residues to contact fluorescence quenching, eventually leading to the decrement of fluorescence intensity and ultraviolet peak. The phenomenon after 40 + 20 kHz 0° treatment was particularly obvious.

3.4.4. Microstructure

The microstructure of SP after ultrasonic treatments is shown in Fig. 5H, and all images are of equal magnification. At 850 magnification power, it was found that the microstructure of untreated SP was loose and fluffy, showing a thin sheet distribution with many micropores. After ultrasonic treatments, surface micropores of SP became significantly larger than those of the Control, and even somewhere torn, especially after 40 + 20 kHz 0° treatment. The connection between micropores was broken, leaving some long or punctiform structures. After ultrasonic treatments, the spatial structure of SP changed.

3.4.5. Thermal stability

The quality loss of temperature function of SP at 35–600 °C was studied by thermogravimetric analysis in Fig. 5I. TG curves were roughly divided into three stages: water evaporation stage, rapid degradation stage and slow degradation stage. In the range of 35–200 °C was the water evaporation stage, including free water, bound water and intramolecular water [74], with some low molecular weight volatile compounds released [75]. The range of 200–480 °C was the main weightlessness stage, which was related to the thermal decomposition of proteins. At the time, the degradations for the Control, 40 kHz, 20 kHz, 40 + 20 kHz 0°, 40 + 20 kHz 30° and 40 + 20 kHz 45° treatment were 65.05%, 67.87%, 71.39%, 68.44%, 71.56% and 69.17%, respectively. Quality loss increased after ultrasonic treatments, indicating that ultrasound reduced the thermal stability of SP, which was similar to the result of [76]. The reason was that enormous shearing force and turbulence formed by ultrasonic cavitation promoted protein molecular structure to change and produced some low molecular weight proteins, while low molecular weight proteins were easier to degrade than high molecular weight proteins, leading to lower thermal stability [10,76]. Slow quality loss at 480–600 °C was associated with the degradation of some stable and complex compounds such as lignin [77]. DTG curves were the first derivative of quality loss curve, representing degradation rate. In Fig. 5J, the first inflection point occurred near 60 °C, corresponding to the first stage of TG curves, namely water evaporation stage. The second inflection point was near 315 °C, which was caused by the rapid degradation of SP. An inflection point at 370 °C might be caused by the low purity of proteins with some impurities, such as aliphatic compounds, and degraded to cause quality loss [77].

3.5. Correlation analysis

Correlation analysis was a statistical method that was used to evaluate the correlation of variables and showed the relationship between indicators [78]. As shown in Fig. 6A, correlation analysis was conducted

on the physicochemical properties of raw soymilk and structural properties of SP. Results displayed that ultrasonic cavitation and micro-jet phenomena improved the permeability of cell membrane, broadened cell channels, and promoted the flowing of content, resulting in the increment of conductivity, SPC, TP and TFC. The similar result was shown in other study [47]. When the ultrasonic cavitation effect was enhanced, the damage degree of cell wall was more severe, the conductivity increased, and the outflow amount of proteins, TP, TFC and other contents increased. Therefore, there was a significant correlation between the conductivity and SPC ($r = 0.53^{***}$), TP ($r = 0.86^{***}$), TFC ($r = 0.89^{***}$). SPC is also related to the beany flavor in Fig. 6A, so SPC has significantly positive correlation with E-nose beneficial ($r = 0.63^{***}$) and E-nose negative ($r = 0.52^{***}$). Particle size of protein was also correlated with E-nose beneficial ($r = 0.48^{***}$) and E-nose negative ($r = 0.42^{***}$), which might be that stronger ultrasonic field increased the degree of protein denaturation and aggregation, and the combination with flavor compounds was destroyed [68]. There was a significant negative correlation between particle size and brightness ($r = -0.85^{***}$), which was due to the increment of particle size of SP, and light reflection in uneven raw soymilk decreased, leading to decrement of brightness ultimately [79]. Ultrasound destroyed cells and plant tissues in cells [53], causing the decomposition of color substances in cells [51], and the color properties of products were affected ultimately. Ultrasonic cavitation also promoted the formation of free radicals and led to enzymatic browning [50], so the stronger the ultrasonic cavitation, the lower the brightness and whiteness, and the higher the yellowness. α-helix, β-sheet, β-turn and random coil represented the protein secondary structure, and the content changes were generally correlated with various indexes. The shear force and micro-jet generated by ultrasonic cavitation destroyed the protein interaction and changed the spatial structure, the groups were exposed, the denaturation and aggregation of proteins were generated with the increment of particle size. On this basis, emulsifying properties, foaming properties, viscosity, surface tension and thermal stability of raw soymilk were changed.

In Fig. 6B, treatments or indicators with the same characteristics are further divided by cluster analysis. 25 indexes were divided into three classes. Class I included 10 indexes such as viscosity (112.214 s^{-1}), solubility, surface tension, random coil, whiteness value, brightness, α-helix, FS, system stability and EAI. Class II contained 10 indexes including turbidity, yellowness, particle size, conductivity, zeta-potential, FC, TFC, TP, ESI, β-sheet, etc. Class III was mainly composed of SPC, E-nose beneficial (W2W), E-nose negative (W5S, W1W), β-turn and thermal stability. In addition, the treated samples were divided into three groups by cluster analysis. The treated group A had the highest abundance in class I, indicating that group A (Control, 40 kHz treatment) obtained the highest value for index in class I. The abundance of group B was the highest in class II, indicating that group B (40 + 20 kHz 0° treatment) obtained the highest value for the index of class II. The abundance of group C was the highest in the class III, indicating that for the class III index, group C (40 + 20 kHz 45°, 20 kHz, 40 + 20 kHz 30° treatment) obtained the highest value.

4. Conclusions

Effects of dual-frequency ultrasonic treatments at different angles on physicochemical properties and flavor of raw soymilk were studied. Furthermore, the spatial structure, microstructure, and thermal stability of SP were analyzed. The ultrasonic field intensity was monitored in time–frequency domain. Results showed that in comparison with single-frequency, dual-frequency ultrasound significantly increased SPC of raw soymilk and was highest after 40 + 20 kHz 45° treatment. The ultrasonic field intensity and spatial peak acoustic intensity were the largest after 40 + 20 kHz 0° treatment. Ultrasonic cavitation changed the spatial structure of SP, and the particle size increased. Emulsification, foaming properties, viscosity, and flavor all changed, while the solubility and thermal stability reduced. Overall, dual-frequency multi-angle ultrasonic treatment increased SPC of raw soymilk and improved its flavor.

CRediT authorship contribution statement

Lei Zhang: Investigation, Data curation, Writing – original draft. **Xue Wang:** Investigation, Data curation, Writing – original draft. **Yang Hu:** Investigation, Data curation, Writing – original draft. **Olugbenga Abiola Fakayode:** Writing – review & editing. **Haile Ma:** Supervision. **Cunshan Zhou:** Supervision. **Zhenyuan Hu:** Investigation, Data curation. **Aiming Xia:** Supervision. **Qun Li:** Supervision.

Declaration of Competing Interest

The authors declare that they have no known competing financial interests or personal relationships that could have appeared to influence the work reported in this paper.

Acknowledgements

This work was supported by the National Natural Science Foundation of China (31801599); District Key Research and Development Program of Dantu (NY2019006).

References

[1] Y.-T. Li, M.-S. Chen, L.-Z. Deng, Y.-Z. Liang, Y.-K. Liu, W. Liu, J. Chen, C.-M. Liu, Whole soybean milk produced by a novel industry-scale micofluidizer system without soaking and filtering, J. Food Eng. 291 (2021) 110228, https://doi.org/10.1016/j.jfoodeng.2020.110228.
[2] C. Cabanos, Y. Matsuoka, N. Maruyama, Soybean proteins/peptides: a review on their importance, biosynthesis, vacuolar sorting, and accumulation in seeds, Pept. 143 (2021) 170598, https://doi.org/10.1016/j.peptides.2021.170598.
[3] T.Y. Hendrawati, K. Audini, Ismiyati, A.I. Ramadhan, H. Gustia, Effects and characterization of different soybean varieties in yield and organoleptic properties of tofu, Results Eng., 11 (2021) 100238, https://doi.org/10.1016/j.rineng.2021.100238.
[4] B. Wang, Q. Zhang, N. Zhang, K.H. Bak, O.P. Soladoye, R.E. Aluko, Y. Fu, Y. H. Zhang, Insights into formation, detection and removal of the beany flavor in soybean protein, Trends Food Sci. Technol. 112 (2021) 336–347, https://doi.org/10.1016/j.tifs.2021.04.018.
[5] N.A. Amirullah, N.Z. Abidin, N. Abdullah, S. Manickam, The ultrasound extract of Pleurotus pulmonarius (Fr.) Quél alleviates metabolic syndromes in hyperlipidaemic Wistar-Kyoto rats fed with a high-fat diet, Biocatal. Agric. Biotechnol., 34 (2021) 102019, https://doi.org/10.1016/j.bcab.2021.102019.
[6] Z.-L. Chen, C. Wang, H. Ma, Y. Ma, J.-K. Yan, Physicochemical and functional characteristics of polysaccharides from okra extracted by using ultrasound at different frequencies, Food Chem. 361 (2021) 130138, https://doi.org/10.1016/j.foodchem.2021.130138.
[7] O.A. Ghazy, M.T. Fouad, H.H. Saleh, A.E. Kholif, T.A. Morsy, Ultrasound-assisted preparation of anise extract nanoemulsion and its bioactivity against different pathogenic bacteria, Food Chem. 341 (2021) 128259, https://doi.org/10.1016/j.foodchem.2020.128259.
[8] Y. Ding, H. Ma, K.e. Wang, S.M.R. Azam, Y. Wang, J. Zhou, W. Qu, Ultrasound frequency effect on soybean protein: Acoustic field simulation, extraction rate and structure, LWT-Food Sci. Technol. 145 (2021) 111320, https://doi.org/10.1016/j.lwt.2021.111320.
[9] S. Jun, M.u. Yaoyao, J. Hui, M. Obadi, C. Zhongwei, X.u. Bin, Effects of single- and dual-frequency ultrasound on the functionality of egg white protein, J. Food Eng. 277 (2020) 109902, https://doi.org/10.1016/j.jfoodeng.2020.109902.
[10] M.A. Malik, C.S. Saini, Rheological and structural properties of protein isolates extracted from dephenolized sunflower meal: Effect of high intensity ultrasound, Food Hydrocolloids 81 (2018) 229–241, https://doi.org/10.1016/j.foodhyd.2018.02.052.
[11] C. Zhao, Z. Chu, Z. Miao, J. Liu, J. Liu, X. Xu, Y. Wu, B. Qi, J. Yan, Ultrasound heat treatment effects on structure and acid-induced cold set gel properties of soybean protein isolate, Food Biosci. 39 (2021) 100827, https://doi.org/10.1016/j.fbio.2020.100827.
[12] R.A. Khaire, A.A. Sunny, P.R. Gogate, Ultrasound assisted ultrafiltration of whey using dual frequency ultrasound for intensified recovery of lactose, Chem. Eng. Process. 142 (2019) 107581, https://doi.org/10.1016/j.cep.2019.107581.
[13] L. Huang, S. Jia, W. Zhang, L. Ma, X. Ding, Aggregation and emulsifying properties of soybean protein isolate pretreated by combination of dual-frequency ultrasound and ionic liquids, J. Mol. Liq. 301 (2020) 112394, https://doi.org/10.1016/j.molliq.2019.112394.
[14] L. Ye, X. Zhu, Y. Liu, Numerical study on dual-frequency ultrasonic enhancing cavitation effect based on bubble dynamic evolution, Ultrason. Sonochem. 59 (2019) 104744, https://doi.org/10.1016/j.ultsonch.2019.104744.

[15] H. Cao, D. Meng, X. Liu, T. Ye, M. Yuan, J. Yu, X. Wu, Y. Li, F. Yin, F. Xu, Extraction of Pb(II) from wheat samples via dual-frequency ultrasound-assisted enzymatic digestion and the mechanisms of its interactions with wheat proteins, Food Chem. 363 (2021) 130247, https://doi.org/10.1016/j.foodchem.2021.130247.
[16] X. Chen, Z. Wang, J. Kan, Polysaccharides from ginger stems and leaves: Effects of dual and triple frequency ultrasound assisted extraction on structural characteristics and biological activities, Food Biosci. 42 (2021) 101166, https://doi.org/10.1016/j.fbio.2021.101166.
[17] H. Lian, C. Wen, J. Zhang, Y. Feng, Y. Duan, J. Zhou, Y. He, H. Zhang, H. Ma, Effects of simultaneous dual-frequency divergent ultrasound-assisted extraction on the structure, thermal and antioxidant properties of protein from Chlorella pyrenoidosa, Algal Res. 56 (2021) 102294, https://doi.org/10.1016/j.algal.2021.102294.
[18] B. Xu, J. Yuan, L. Wang, F. Lu, B. Wei, R.S.M. Azam, X. Ren, C. Zhou, H. Ma, B. Bhandari, Effect of multi-frequency power ultrasound (MFPU) treatment on enzyme hydrolysis of casein, Ultrason. Sonochem. 63 (2020) 104930, https://doi.org/10.1016/j.ultsonch.2019.104930.
[19] S. Merouani, O. Hamdaoui, Y. Rezgui, M. Guemini, Effects of ultrasound frequency and acoustic amplitude on the size of sonochemically active bubbles-Theoretical study, Ultrason. Sonochem. 20 (3) (2013) 815–819, https://doi.org/10.1016/j.ultsonch.2012.10.015.
[20] H. Delmas, N.T. Le, L. Barthe, C. Julcour-Lebigue, Optimization of hydrostatic pressure at varied sonication conditions-power density, intensity, very low frequency-for isothermal ultrasonic sludge treatment, Ultrason. Sonochem. 25 (2015) 51–59, https://doi.org/10.1016/j.ultsonch.2014.08.011.
[21] K.L. Tan, S.H. Yeo, Bubble dynamics and cavitation intensity in milli-scale channels under an ultrasonic horn, Ultrason. Sonochem. 58 (2019) 104666, https://doi.org/10.1016/j.ultsonch.2019.104666.
[22] L. Zhang, Y. Hu, B. Wang, X. Xu, A.E.A. Yagoub, O.A. Fakayode, H. Ma, C. Zhou, Effect of ultrasonic pretreatment monitored by real-time online technologies on dried preparation time and yield during extraction process of okra pectin, J. Sci. Food Agric. 101 (10) (2021) 4361–4372, https://doi.org/10.1002/jsfa.v101.1010.1002/jsfa.11076.
[23] J. Du, F. Chen, Cavitation dynamics and flow aggressiveness in ultrasonic cavitation erosion, Int. J. Mech. Sci. 204 (2021) 106545, https://doi.org/10.1016/j.ijmecsci.2021.106545.
[24] V.C. Kaharso, B. Muhoza, X. Kong, Y. Hua, C. Zhang, Quality improvement of soymilk as influenced by anaerobic grinding method and calcium addition, Food Biosci. 42 (2021) 101210, https://doi.org/10.1016/j.fbio.2021.101210.
[25] Z. Guo, Z. Huang, Y. Guo, B. Li, W. Yu, L. Zhou, L. Jiang, F. Teng, Z. Wang, Effects of high-pressure homogenization on structural and emulsifying properties of thermally soluble aggregated kidney bean (Phaseolus vulgaris L.) proteins, Food Hydrocolloids 119 (2021) 106835, https://doi.org/10.1016/j.foodhyd.2021.106835.
[26] H. Li, F. Li, X. Wu, W. Wu, Effect of rice bran rancidity on the emulsion stability of rice bran protein and structural characteristics of interface protein, Food Hydrocolloids 121 (2021) 107006, https://doi.org/10.1016/j.foodhyd.2021.107006.
[27] Y. Zhu, S. Fu, C. Wu, B. Qi, F. Teng, Z. Wang, Y. Li, L. Jiang, The investigation of protein flexibility of various soybean cultivars in relation to physicochemical and conformational properties, Food Hydrocolloids 103 (2020) 105709, https://doi.org/10.1016/j.foodhyd.2020.105709.
[28] P.K. Smith, R.I. Krohn, G.T. Hermanson, A.K. Mallia, F.H. Gartner, M. D. Provenzano, E.K. Fujimoto, N.M. Goeke, B.J. Olson, D.C. Klenk, Measurement of protein using bicinchoninic acid, Anal. Biochem. 150 (1) (1985) 76–85, https://doi.org/10.1016/0003-2697(85)90442-7.
[29] L. Sha, A.O. Koosis, Q. Wang, A.D. True, Y.L. Xiong, Interfacial dilatational and emulsifying properties of ultrasound-treated pea protein, Food Chem. 350 (2021) 129271, https://doi.org/10.1016/j.foodchem.2021.129271.
[30] Y. Shen, D. Zhu, P. Xi, T. Cai, X. Cao, H.e. Liu, J. Li, Effects of temperature-controlled ultrasound treatment on sensory properties, physical characteristics and antioxidant activity of cloudy apple juice, LWT-Food Sci. Technol. 142 (2021) 111030, https://doi.org/10.1016/j.lwt.2021.111030.
[31] X. Song, X. Yu, C. Zhou, B. Xu, L.i. Chen, A. ElGasim A. Yagoub, O.C. Emeka, H. Wahia, Conveyor belt catalytic infrared as a novel apparatus for blanching processing applied to sweet potatoes in the industrial scale, LWT-Food Sci. Technol. 149 (2021) 111827, https://doi.org/10.1016/j.lwt.2021.111827.
[32] C.-C. Zhao, J.-K. Lu, K. Ameer, Effects of tofu whey powder on the quality attributes, isoflavones composition and antioxidant activity of wheat flour pan bread, LWT-Food Sci. Technol. 143 (2021) 111166, https://doi.org/10.1016/j.lwt.2021.111166.
[33] Y. Feng, B. Xu, A. ElGasim A. Yagoub, H. Ma, Y. Sun, X. Xu, X. Yu, C. Zhou, Role of drying techniques on physical, rehydration, flavor, bioactive compounds and antioxidant characteristics of garlic, Food Chem. 343 (2021) 128404, https://doi.org/10.1016/j.foodchem.2020.128404.
[34] L. Li, H. He, D. Wu, D. Lin, W. Qin, D. Meng, R. Yang, Q. Zhang, Rheological and textural properties of acid-induced soybean protein isolate gel in the presence of soybean protein isolate hydrolysates or their glycosylated products, Food Chem. 360 (2021) 129991, https://doi.org/10.1016/j.foodchem.2021.129991.
[35] B. Zhou, J.T. Tobin, S. Drusch, S.A. Hogan, Interfacial properties of milk proteins: A review, Adv. Colloid Interface Sci. 295 (2021) 102347, https://doi.org/10.1016/j.cis.2020.102347.
[36] Z. Ren, X. Yu, A.E.A. Yagoub, O.A. Fakayode, H. Ma, Y. Sun, C. Zhou, Combinative effect of cutting orientation and drying techniques (hot air, vacuum, freeze and catalytic infrared drying) on the physicochemical properties of ginger (Zingiber officinale Roscoe), LWT-Food Sci. Technol. 144 (2021) 111238, https://doi.org/10.1016/j.lwt.2021.111238.
[37] L. Xu, W. yan, M.i. Zhang, X. Hong, Y. Liu, J. Li, Application of ultrasound in stabilizing of Antarctic krill oil by modified chickpea protein isolate and ginseng saponin, LWT-Food Sci. Technol. 149 (2021) 111803, https://doi.org/10.1016/j.lwt.2021.111803.
[38] J. Ye, L. Deng, Y. Wang, D.J. McClements, S. Luo, C. Liu, Impact of rutin on the foaming properties of soybean protein: Formation and characterization of flavonoid-protein complexes, Food Chem. 362 (2021) 130238, https://doi.org/10.1016/j.foodchem.2021.130238.
[39] L. Cheng, X.-a. Yang, M.-T. Shi, W.-B. Zhang, Rapid extraction of arsenic species from traditional Chinese herbal by dual-frequency ultrasound-assisted enzymatic digestion prior to spectral analysis, J. Chromatogr. A 1619 (2020) 460915, https://doi.org/10.1016/j.chroma.2020.460915.
[40] L.R. Huang, W.X. Zhang, X.N. Ding, Z.F. Wu, Y.L. Li, Effects of dual-frequency ultrasound with different energy irradiation modes on the structural and emulsifying properties of soy protein isolate, Food Bioprod. Process. 123 (2020) 419–426, https://doi.org/10.1016/j.fbp.2020.07.021.
[41] S. Yan, J. Xu, S. Zhang, Y. Li, Effects of flexibility and surface hydrophobicity on emulsifying properties: Ultrasound-treated soybean protein isolate, LWT-Food Sci. Technol. 142 (2021) 110881, https://doi.org/10.1016/j.lwt.2021.110881.
[42] A.B. Khatkar, A. Kaur, S.K. Khatkar, Restructuring of soy protein employing ultrasound: Effect on hydration, gelation, thermal, in-vitro protein digestibility and structural attributes, LWT-Food Sci. Technol. 132 (2020) 109781, https://doi.org/10.1016/j.lwt.2020.109781.
[43] A.B. Tomé Constantino, E.E. Garcia-Rojas, Modifications of physicochemical and functional properties of amaranth protein isolate (Amaranthus cruentus BRS Alegria) treated with high-intensity ultrasound, J. Cereal Sci. 95 (2020) 103076, https://doi.org/10.1016/j.jcs.2020.103076.
[44] M.L. Rojas, T.S. Leite, M. Cristianini, I.D. Alvim, P.E.D. Augusto, Peach juice processed by the ultrasound technology: Changes in its microstructure improve its physical properties and stability, Food Res. Int. 82 (2016) 22–33, https://doi.org/10.1016/j.foodres.2016.01.011.
[45] R.P. Gao, F.Y. Ye, Y.L. Wang, Z.Q. Lu, M.Y. Yuan, G.H. Zhao, The spatial-temporal working pattern of cold ultrasound treatment in improving the sensory, nutritional and safe quality of unpasteurized raw tomato juice, Ultrason. Sonochem. 56 (2019) 240–253, https://doi.org/10.1016/j.ultsonch.2019.04.013.
[46] J. Wang, Q. Liu, B. Xie, Z. Sun, Effect of ultrasound combined with ultraviolet treatment on microbial inactivation and quality properties of mango juice, Ultrason. Sonochem. 64 (2020) 105000, https://doi.org/10.1016/j.ultsonch.2020.105000.
[47] J. Wang, S.K. Vanga, V. Raghavan, High-intensity ultrasound processing of kiwifruit juice: Effects on the ascorbic acid, total phenolics, flavonoids and antioxidant capacity, LWT-Food, Sci. Technol. 107 (2019) 299–307, https://doi.org/10.1016/j.lwt.2019.03.024.
[48] L.E. Ordonez-Santos, J. Martinez-Giron, M.E. Arias-Jaramillo, Effect of ultrasound treatment on visual color, vitamin C, total phenols, and carotenoids content in Cape gooseberry juice, Food Chem. 233 (2017) 96–100, https://doi.org/10.1016/j.foodchem.2017.04.114.
[49] E.A. Rios-Romero, L.A. Ochoa-Martínez, L.A. Bello-Pérez, J. Morales-Castro, A. Quintero-Ramos, J.A. Gallegos-Infante, Effect of ultrasound and steam treatments on bioaccessibility of beta-carotene and physicochemical parameters in orange-fleshed sweet potato juice, Heliyon 7 (2021), e06632, https://doi.org/10.1016/j.heliyon.2021.e06632.
[50] Q.A. Zhang, T.T. Wang, Effect of ultrasound irradiation on the evolution of color properties and major phenolic compounds in wine during storage, Food Chem. 234 (2017) 372–380, https://doi.org/10.1016/j.foodchem.2017.05.022.
[51] F.F. de Araújo D. de Paulo Farias I.A. Neri-Numa F.L. Dias-Audibert J. Delafiori F. G. de Souza R.R. Catharino C.K. do Sacramento, G.M. Pastore, Influence of high-intensity ultrasound on color, chemical composition and antioxidant properties of araca-boi pulp Food Chem. 127747 338 (2021) 10.1016/j.foodchem.2020.127747.
[52] J. Wang, J. Wang, J.H. Ye, S.K. Vanga, V. Raghavan, Influence of high-intensity ultrasound on bioactive compounds of strawberry juice: Profiles of ascorbic acid, phenolics, antioxidant activity and microstructure, Food Control 96 (2019) 128–136, https://doi.org/10.1016/j.foodcont.2018.09.007.
[53] N.T. Flores-Jiménez, J.A. Ulloa, J.E.U. Silvas, J.C.R. Ramírez, P.R. Ulloa, P.U. B. Rosales, Y.S. Carrillo, R.G. Leyva, Effect of high-intensity ultrasound on the compositional, physicochemical, biochemical, functional and structural properties of canola (Brassica napus L.) protein isolate, Food Res. Int. 121 (2019) 947–956, https://doi.org/10.1016/j.foodres.2019.01.025.
[54] Y.Y. Chang, D. Li, L.J. Wang, C.H. Bi, B. Adhikari, Effect of gums on the rheological characteristics and microstructure of acid-induced SPI-gum mixed gels, Carbohydr. Polym. 108 (2014) 183–191, https://doi.org/10.1016/j.carbpol.2014.02.089.
[55] A.R. Salve, K. Pegu, S.S. Arya, Comparative assessment of high-intensity ultrasound and hydrodynamic cavitation processing on physico-chemical properties and microbial inactivation of peanut milk, Ultrason. Sonochem. 59 (2019) 104728, https://doi.org/10.1016/j.ultsonch.2019.104728.
[56] M. Dissanayake, S. Liyanaarachchi, T. Vasiljevic, Functional properties of whey proteins microparticulated at low pH, J. Dairy Sci. 95 (4) (2012) 1667–1679, https://doi.org/10.3168/jds.2011-4823.
[57] J. Chen, X. Zhang, Y. Chen, X. Zhao, B. Anthony, X. Xu, Effects of different ultrasound frequencies on the structure, rheological and functional properties of myosin: Significance of quorum sensing, Ultrason. Sonochem. 69 (2020) 105268, https://doi.org/10.1016/j.ultsonch.2020.105268.
[58] J. Wang, X. Na, W.B. Navicha, C. Wen, W. Ma, X. Xu, C. Wu, M. Du, Concentration-dependent improvement of gelling ability of soy proteins by preheating or

ultrasound treatment, LWT-Food Sci. Technol. 134 (2020) 110170, https://doi.org/10.1016/j.lwt.2020.110170.
[59] K. Li, Y. Li, C.-L. Liu, L. Fu, Y.-Y. Zhao, Y.-Y. Zhang, Y.-T. Wang, Y.-H. Bai, Improving interfacial properties, structure and oxidative stability by ultrasound application to sodium caseinate prepared pre-emulsified soybean oil, LWT-Food Sci. Technol. 131 (2020) 109755, https://doi.org/10.1016/j.lwt.2020.109755.
[60] C. Amine, J. Dreher, T. Helgason, T. Tadros, Investigation of emulsifying properties and emulsion stability of plant and milk proteins using interfacial tension and interfacial elasticity, Food Hydrocolloids 39 (2014) 180–186, https://doi.org/10.1016/j.foodhyd.2014.01.001.
[61] F. Wang, Y. Zhang, L. Xu, H. Ma, An efficient ultrasound-assisted extraction method of pea protein and its effect on protein functional properties and biological activities, LWT-Food Sci. Technol. 127 (2020) 109348, https://doi.org/10.1016/j.lwt.2020.109348.
[62] H. Liu, J. Zhang, H. Wang, Q. Chen, B. Kong, High-intensity ultrasound improves the physical stability of myofibrillar protein emulsion at low ionic strength by destroying and suppressing myosin molecular assembly, Ultrason. Sonochem. 74 (2021) 105554, https://doi.org/10.1016/j.ultsonch.2021.105554.
[63] A. Martínez-Velasco, C. Lobato-Calleros, B.E. Hernández-Rodríguez, A. Román-Guerrero, J. Alvarez-Ramirez, E.J. Vernon-Carter, High intensity ultrasound treatment of faba bean (Vicia faba L.) protein: Effect on surface properties, foaming ability and structural changes, Ultrason. Sonochem. 44 (2018) 97–105, https://doi.org/10.1016/j.ultsonch.2018.02.007.
[64] T. Xiong, W.F. Xiong, M.T. Ge, J.H. Xia, B. Li, Y.J. Chen, Effect of high intensity ultrasound on structure and foaming properties of pea protein isolate, Food Res. Int. 109 (2018) 260–267, https://doi.org/10.1016/j.foodres.2018.04.044.
[65] Y.J. Zhao, C.T. Wen, Y.Q. Feng, J.X. Zhang, Y.Q. He, Y.Q. Duan, H.H. Zhang, H. L. Ma, Effects of ultrasound-assisted extraction on the structural, functional and antioxidant properties of Dolichos lablab L, Protein, Process Biochem. 101 (2021) 274–284, https://doi.org/10.1016/j.procbio.2020.11.027.
[66] A.T. Mustapha, C. Zhou, Novel assisted/unassisted ultrasound treatment: Effect on respiration rate, ethylene production, enzymes activity, volatile composition, and odor of cherry tomato, LWT-Food Sci. Technol. 149 (2021) 111779, https://doi.org/10.1016/j.lwt.2021.111779.
[67] K. Wang, S.D. Arntfield, Interaction of selected volatile flavour compounds and salt-extracted pea proteins: Effect on protein structure and thermal-induced gelation properties, Food Hydrocolloids 51 (2015) 383–394, https://doi.org/10.1016/j.foodhyd.2015.05.044.
[68] J. Zhang, D.C. Kang, W.G. Zhang, J.M. Lorenzo, Recent advantage of interactions of protein-flavor in foods: Perspective of theoretical models, protein properties and extrinsic factors, Trends Food Sci. Technol. 111 (2021) 405–425, https://doi.org/10.1016/j.tifs.2021.02.060.
[69] Xin Xu Lei Zhang Yabin Feng Cunshan Zhou Abu ElGasim A. Yagoub Hafida Wahia Haile Ma Jin Zhang Yanhui Sun 70 2021 105300 10.1016/j.ultsonch.2020.105300.
[70] Z. Zhang, Y. Wang, H. Jiang, C. Dai, Z. Xing, B. Kumah Mintah, M. Dabbour, R. He, H. Ma, Effect of dual-frequency ultrasound on the formation of lysinoalanine and structural characterization of rice dreg protein isolates, Ultrason. Sonochem. 67 (2020) 105124, https://doi.org/10.1016/j.ultsonch.2020.105124.
[71] L.Z. Jiang, J. Wang, Y. Li, Z.J. Wang, J. Liang, R. Wang, Y. Chen, W.J. Ma, B.Q. Qi, M. Zhang, Effects of ultrasound on the structure and physical properties of black bean protein isolates, Food Res. Int. 62 (2014) 595–601, https://doi.org/10.1016/j.foodres.2014.04.022.
[72] S. Huang, Y. Li, C. Li, S. Ruan, S.M. Roknul Azam, N. Ou Yang, X. Ye, Y. Wang, H. Ma, Effects of ultrasound-assisted sodium bisulfite pretreatment on the preparation of cholesterol-lowering peptide precursors from soybean protein, Int. J. Biol. Macromol. 183 (2021) 295–304, https://doi.org/10.1016/j.ijbiomac.2021.04.125.
[73] A.B. Khatkar, A. Kaur, S.K. Khatkar, N. Mehta, Characterization of heat-stable whey protein: Impact of ultrasound on rheological, thermal, structural and morphological properties, Ultrason. Sonochem. 49 (2018) 333–342, https://doi.org/10.1016/j.ultsonch.2018.08.026.
[74] X. Xu, L. Zhang, Abu.ElGasim.A. Yagoub, X. Yu, H. Ma, C. Zhou, Effects of ultrasound, freeze-thaw pretreatments and drying methods on structure and functional properties of pectin during the processing of okra, Food Hydrocolloids 120 (2021) 106965, https://doi.org/10.1016/j.foodhyd.2021.106965.
[75] L.N. Yu, W.Q. Yang, J. Sun, C.S. Zhang, J. Bi, Q.L. Yang, Preparation, characterisation and physicochemical properties of the phosphate modified peanut protein obtained from Arachin Conarachin L, Food Chem. 170 (2015) 169–179, https://doi.org/10.1016/j.foodchem.2014.08.047.
[76] N.A. Mir, C.S. Riar, S. Singh, Physicochemical, molecular and thermal properties of high-intensity ultrasound (HIUS) treated protein isolates from album (Chenopodium album) seed, Food Hydrocolloids 96 (2019) 433–441, https://doi.org/10.1016/j.foodhyd.2019.05.052.
[77] Y. Feng, C. Ping Tan, C. Zhou, Abu.ElGasim.A. Yagoub, B. Xu, Y. Sun, H. Ma, X. Xu, X. Yu, Effect of freeze-thaw cycles pretreatment on the vacuum freeze-drying process and physicochemical properties of the dried garlic slices, Food Chem. 324 (2020) 126883, https://doi.org/10.1016/j.foodchem.2020.126883.
[78] J.K. Kim, E.-H. Kim, I. Park, B.-R. Yu, J.D. Lim, Y.-S. Lee, J.-H. Lee, S.-H. Kim, I.-M. Chung, Isoflavones profiling of soybean [Glycine max (L.) Merrill] germplasms and their correlations with metabolic pathways, Food Chem. 153 (2014) 258–264, https://doi.org/10.1016/j.foodchem.2013.12.066.
[79] J. Wang, M. Zhang, S. Devahastin, Y. Liu, Influence of low-temperature ball milling time on physicochemical properties, flavor, bioactive compounds contents and antioxidant activity of horseradish powder, Adv. Powder Technol. 31 (3) (2020) 914–921, https://doi.org/10.1016/j.apt.2019.12.011.